Thesis/
Reports
Sorooshian

ARID LANDS WATER RESOURCES MONITORING FOR OUTLIER EVENTS ON UNGAGED WATERSHEDS USING RADAR RAINFALL MEASUREMENTS

FINAL REPORT

ARID LANDS WATER RESOURCES MONITORING FOR OUTLIER EVENTS ON UNGAGED WATERSHEDS USING RADAR RAINFALL MEASUREMENTS

Research Grant No. 28-G3-696

between

Arizona Board of Regents
Department of Hydrology and Water Resources

and

Rocky Mountain Forest and Range Experiment Station

U.S. Investigators[1]

Prof. Soroosh Sorooshian (P.I.)
Head, Dept. of Hydrology
and Water Resources
University of Arizona
Tucson, AZ 85721

Prof. Simon Ince
Dept. of Hydrology
and Water Resources
University of Arizona
Tucson, AZ 85721

Dr. David C. Goodrich
Research Hydraulic Engr.
Southwest Watershed Research
Center
USDA-ARS
Tucson, AZ 85719

Israeli Investigators[2]

Dr. Joseph Morin
Chief Research Advisor
Soil Conservation Dept.
Soil Erosion Research Station
Rupin Institute Post
Emek Hefer 60960
ISRAEL

Dr. Rami Garti
Director
Soil Erosion Research Station
Rupin Institute Post
Emek Hefer 60960
ISRAEL

Prof. Daniel Rosenfeld
Dept. of Atmospheric Sci.
Institute of Earth Sciences
The Hebrew Univ. of Jerusalem
Jerusalem 91904, ISRAEL

[1]Ibrahim El-Shinaway, currently at the Water Research Center, Research Institute of Water Resources, Cairo, Egypt, also contributed to the final report.

[2]Eyal Amitai, The Hebrew University of Jerusalem, Jerusalem, Israel, also contributed to the final report.

December 1994.

LIBRARY COPY
ROCKY MTN. FOREST & RANGE
EXPERIMENT STATION

ABSTRACT

Effective monitoring of water resources in arid land regions is critical for both restoration efforts and efficient existing land use. Frequent representative sampling of a large range of runoff event sizes requires substantial budgetary resources and is even more difficult in arid and semi-arid areas, where rainfall events are typically more variable. However, for a fixed time period, over a large region with many watersheds, it is more likely to encounter some extreme, or outlier, events on one or more of the watersheds then for single well-instrumented watershed. Identifying and analyzing data from these isolated watersheds can greatly reduce the time and expenditure required for obtaining long-term data from a permanently instrumented watershed. Several components of a system to acquire and analyze hydrometeorological data from isolated watersheds were tested by a Israeli and U.S. team. This Israeli team applied a new method of radar-rainfall estimation over several catchment areas in central Israel known as the "Window Probability Matching Method (WPMM)". Comparison of daily rainfall measurements by rain gauges with radar-rainfall estimates above the gauges demonstrated good agreement. The standard error of radar estimated rainfall was only 7% for a storm with a total average accumulation of 328 mm. The U.S. team conducted a comparison of indirect peak discharge measurements to peak runoff estimates from supercritical flumes in ephemeral channels of a semi-arid experimental watershed. Four indirect measurements compared very well with flume observations. Uncertainty analysis for the impacts of roughness and water slope variations on indirect peak estimates indicated that substantial variation in peak discharge can result from realistic variations in roughness and slope as interpreted from the field data. The uncertainty of indirect peak discharge estimation was then compared to rainfall-runoff modeling results from a nearby subwatershed. The comparison indicated that high spatial resolution rainfall data and a distributed runoff model may be able to predict peak runoff rates with comparable accuracy to indirect measurements. However, a larger data set and more extensive modeling analysis will be required to draw any strong conclusions. If this conclusion does hold, the possibility exists to develop an arid lands water resources monitoring system for outlier events on ungaged watersheds using radar-rainfall measurements coupled with a distributed rainfall-runoff model. The potential savings by properly utilizing these tools is important to every country and absolutely vital to developing countries. This will enable more effective arid land water utilization for current activities as well as restoration efforts.

General Project Objective

The general project objective was to develop a method for utilizing modern techniques which enable more rapid and economical means of gathering and analyzing data resulting from random flash flood events based on the acquisition, analysis, and documentation of data obtained during outlier rainfall and runoff events. To attack this general objective within the awarded budget, the project addressed several key components of a system to collect outlier rainfall and runoff event information through specific U.S. and Israeli objectives.

Specific Israeli and United States Project Objectives

A. Israel Team

The primary objective for this part of the research was to implement a new window probability matching method (WPMM) to compute rainfall intensities from radar reflectivity and test the method with observed Israeli radar and raingage data. In addition, to illustrate how such accurate radar estimated rainfall with good temporal and spatial resolution might be used for hydrological purposes. This is demonstrated by several case studies. It is believed that the WPMM is far superior to the current class of algorithms that will be used to process NEXRAD radar data, particularly in a semi-arid environment dominated by convective rainfall.

B. United States Team

The primary objective for this part of the research was to quantify the uncertainty associated with peak flood discharge estimates obtained from post-flood, indirect methods in ephemeral regions. This was accomplished by comparing the indirect measurements to direct stage-discharge measurement using special runoff flumes of the USDA-ARS Walnut Gulch Experimental Watershed. This is required because the specially designed and instrumented runoff flumes in Walnut Gulch can not be economically constructed and installed over wide regions to measure outlier events. The indirect discharge measurement uncertainty will be compared to typical rainfall-runoff model estimate uncertainty.

General Premise: If a rainfall-runoff model, using improved radar-rainfall estimates, predicts peak runoff rate as accurately as post-storm, indirect discharge measurements than, a viable system can be assembled using the radar data and a runoff model to inexpensively collect outlier flood data over a wide region.

ISRAELI TEAM RESULTS

INTRODUCTION

To obtain rainfall measurements over large areas, only weather radar can provide a feasible way for obtaining such data. Great variability exists, however, between rain intensities (R) and the radar echo intensity (Z) reflected by the precipitation. This variability prevented extensive applications of weather radar for hydrological purposes. The main reasons for this variability are: (a) differences in rain drop size distribution (DSD) of different rain regimes, such as convective, stratiform, and shallow warm rain; (b) differences in the DSD produced by the same convective cloud during its lifecycle; (c) strong horizontal gradients of the rain intensities, which causes large bias errors due to partial radar beam filling; (d) vertical variations of the precipitation in the clouds (the radar beam spreads and the radar horizon is elevated above the surface with increasing distance). These reasons severely limit the usefulness of radar for hydrometeorological applications.

Recent methodological advances in rainfall measurement by application of conventional weather radars, makes it possible to account for much of the variations in the precipitation radar echo intensity - rain intensity relations. This new technology significantly improve the accuracy of the estimated radar rainfall. This method, known as the "Window Probability Matching Method (WPMM)", was applied to radar measurements over several catchment areas in central Israel.

The Importance of Rainfall Measurements with Radar

Accurate measurements of rain intensities with good spatial and temporal resolution is important for many fields. Ecology, agriculture, civil engineering, in general, and hydrology, in particular, can gain substantial benefits from these measurements. Rainfall-runoff relationships are a very important field in hydrology. Information on peak discharge and storm runoff volumes are essential for many civil engineering construction projects, such as roads, bridges, dams, reservoirs, drainage and flood control Tillage practice and water harvesting in semi-arid regions depend critically on these relationships (Morin and Sharon, 1993).

For most hydrological purposes, rainfall is usually determined from a sparse network of rain gauges. Rain gauges sample rain fields at distinct points, and therefore do not represent accurately the spatial distribution of rainfall, especially in convective situations. Satisfactory temporal (5 minutes) and spatial (1 km^2) resolution of rainfall is achievable, in principle, over large areas by use of meteorological radar.

Deficiencies of Currently Available Methods of Radar Rainfall Measurement

Rainfall measurements with radar is a common practice for decades. Low accuracy prevented extensive applications of weather radar for hydrological purposes. It is generally believed that not much can be done to make a significant improvement of the accuracy of the radar rain measurements. In this research we develop a method that show promise for significant such

improvement. In order to appreciate this, following is a detailed account of the reasons causing variability between rain intensities (R) and the radar echo intensity (Z) reflected by the precipitation.

Differences in Rain Drop Size Distribution (DSD) of Different Rain Regimes

The methodology of rainfall measurement with radar was based from its beginning on the theoretical relations between rain drop size distribution (DSD) and the radar reflectivity factor (e.g., Marshall and Palmer, 1948). The relationship was given in the form of a power law

$$Z = KR^{\alpha} \qquad (1)$$

where R is the rain intensity [mm h^{-1}] and Z is the reflectivity factor [mm^3m^{-6}]. Hundreds of such Z-R power law relationships were published since then, with large differences of up to a factor of 5 between rain intensities related to the same reflectivity. Many of these Z-R relationships are cited by Battan in pages 90-92 of his book (1973). Geometrical and timing errors made direct derivations of Z-R relationships from point measurements of radar and rain gauges impractical, except at very close ranges, where general agreement with the DSD-based Z-R relationships was found, as was first shown by Joss et al. (1968, 1970). Therefore, the common approach was to estimate the rain rate by a power law that was based on a "representative" DSD, and then apply a calibration correction in an effort to minimize the differences between the radar integrated rainfall and that obtained from rain gauges (Wilson and Brandes, 1979).

Stout and Mueller (1968), in their survey of Z-R relationships, noted that the large variations of these relationships were primarily associated with differences of geographical locality. In addition, they noted that at one locality "different types of rain or different synoptic conditions" could lead to differences in the order of 150% in the radar estimated rainfall.

Joss et al. (1970) proposed that the characteristics of the echoes could be used to identify the character of the rain. Battan (1973) commented on that: "This information would allow the selection of an appropriate Z-R equation. If this is done automatically by means of computers it should be possible to increase the accuracy of radar measurements of rainfall." The present research is a step towards the realization of Battan's vision.

Variations of Ze-R Due to Distortion of Z

Large differences often exist between the true reflectivity (Z) field and the radar observed reflectivity (Ze) field, which invalidate the use of DSD based Z-R relationships. There are two major sources for these differences:

a) The radar beam spreading, that convolves the radar beam pattern with the true reflectivity field (Donaldson, 1964).

b) The high frequency fluctuations of Ze due to random interference of the echoes reflected from the individual particles (Rogers, 1971).

The effects of these two factors on Z-R relations and area integrated rainfall were shown to be significant in convective rainfall, which is characterized by large horizontal reflectivity gradients (Zawadzki, 1973; Rosenfeld et al. 1992). In agreement with this theory, Klazura (1981) has shown empirically that large radar overestimates were obtained in high rain rate gradient storms.

Variations with Height

Reflectivities are changed with height differently for different rain types. Konrad (1978) and Szoke et al., (1986) classified cloud types by their vertical reflectivity profiles, and according to these studies, reflectivity decreases very rapidly with height in shallow tropical clouds, which produce rain mainly by warm processes. The reflectivity of deep and highly convective clouds remains constant or even increases to heights greater than the freezing level. In stratiform rainfall the reflectivity does not change much below the freezing level, and decreases rapidly above it.

Due to the increasing height of the radar beam with range, each such rain type has its own distinct dependence of the Ze-R relationships on the range and on the freezing level. Rosenfeld et al. (1992) have shown that Ze-R relations change with range in a complex way, which greatly differs for different rain types.

Variation within the Life Cycle of a Cloud

Ze-R relationship of a cloud can significantly vary throughout its life cycle. Rain starts with rain of relatively few large drops, and ends as more smaller drops. Rain starts as highly localized showers, with strong gradients, and ends as a wide spread rain. Rain from a specific cloud may start as convective and end as stratiform, with their distinct differences of DSD. Therefore, a single Z-R relationship cannot possibly provide accurate point estimates of convective rainfall. These large, seemingly random, variability in the Ze-R relationships have till now excluded accurate radar rainfall estimation over small areas for short durations.

NEXRAD - The Next Generation of Weather Radars

The U.S. National Weather Service is modernizing the weather radar network, with the new WSR-88D radar (NEXRAD). The nexrad is a radar of very high quality of signal processing, ground clutter rejection and reliability of data. The NEXRAD has a sweet of algorithms for various applications, including rainfall estimate. The NEXRAD rain algorithms are quite simple conceptually. R is converted from **Z using fixed Z-R power law** that is corrected every hour by the bias between one hour integrated rainfall from a rain gauge network.

Deficiencies of NEXRAD rainfall measurement methods

The NEXRAD rain algorithms are optimized at providing correct integral rain depth only. The same integral rain depth can be obtained with infinite number of different Z-R relations, which can produce **very different radar measured rain intensities.** Another problem comes from the hourly bias correction procedure. As explained in the previous section, small time-space domain measurements of rainfall with radar are highly inaccurate. Therefore, taking several such measurements in several points (over rain gauges) for one hour is likely to do more harm than good in large fraction of the instances.

The Window Probability Matching Method (WPMM)

Recent methodological advances in the technology of rainfall measurement with conventional weather radars (Rosenfeld et al. 1994a, 1994b and 1994c), obtained by the so-called Window Probability Matching Method (WPMM), makes it possible to account for much of the variations of the Ze-R relations and thus significantly improve the accuracy of the estimated radar rainfall. The main steps in the WPMM are as follows:

1) Dividing the radar observed reflectivity (Ze) field into small windows centered over the poi rainfall is to be estimated.
2) Analyzing the 3-dimensional structure of the Ze field within the window, and calculating the values of several parameters which explain the variability in the Ze-R relationships.
3) Using Ze and R values from windows which are collocated and synchronized with rain gauges to establish Ze-R relationships for each set of rain type parameters separately. This Ze-R relation is done by matching the cumulative probabilities of the Ze and R, obtained from all of the windows. In practice, Ze and R having the same cumulative percentile are related to each other.
4) Application of the WPMM requires analysis of the vicinity (window) of each point for its rain type classification parameters, followed by applying the appropriate Ze-R relationships.

The Way WPMM Can Solve Deficiencies in the Conventional Methods

The Ze-R relations obtained by the WPMM, by the fact that they are curved lines in log-log space, can translate the observed reflectivities to rain intensities more accurately than any power law Z-R relation because they are able to account for the true shape of the Ze-R relations and not artificially enforce a straight line approximation. This results in increased accuracy of the estimated rain intensities, beyond the increased accuracy of the integrated rainfall.

Ze-R sets can be found for each rain type separately, as defined by the 3-D reflectivity structure in the radar field window. The application of such a Z-R set, assuming that the radar calibration is constant with time, takes into account the variability of conditions in time and space, and therefore capable of much higher accuracy over all scales. This approach does not require

stringent real time calibration with rain gauges. In addition, the classification into rain cloud types has an intrinsic scientific value.

The primary objective of this research is to implement the WPMM to compute rainfall intensities, test the method with observed Israeli radar and raingage data, and assess how the rainfall estimates might be used for hydrological purposes.

THE STUDY AREA

The research area is the coastal plain of central Israel (see map 1), up to a distance of 80 km from the radar, which is located at Ben-Gurion Airport, 10 km to the east of Tel-Aviv. The Ze-R relationships were obtained from the radar data and a network of 22 recording rain gauges, using the WPMM technique. All the available data (which included most of the rainfall) from the 1991/92 rainy season were analyzed according to this method. These Ze-R relationships were applied to the heavy rain storm that began on November 28 and ended on December 4, 1991. Detailed rain maps with 1 km^2 spatial resolution and 5-minute time resolution were produced for all the study area.

AREAL RAINFALL DISTRIBUTION DATA AND EVALUATION

In this section, the distribution of rainfall intensity and amount is presented for a target area of 20x20 km^2. The area is located 30 km south of Tel Aviv, in the central plain of the coastal region. Daily rainfall is defined as a 24 hour accumulation starting and ending at 8:00 a.m. LST. The rainfall is attributed to the starting date. Plate 1 demonstrates the Nov. 29, 1991 rainfall amount, as analyzed for 400 grid points, each one 1 km^2. The location of the five rainfall recorders, A, B, C, D and E, is indicated on the plate. Spatial rainfall amount variability is indicated by the different colors.

The distribution of the daily rain depth for the Yavne watershed is illustrated in Plate 2, which demonstrates the large areal variability, even for this small 15 km^2 watershed located within the target area. The tremendous spatial variability in space and time of the rainfall intensities is illustrated by Plates 3 and 4 for the Yavne region. Intensity rates in mm/hr are inserted in each of the 1 km^2 grid points. The only operating rain recorder in the watershed is marked by the letter A, which marks its exact location. Assuming the radar estimated rainfall to be true, we can see that this recorder did not sense the high rainfall intensity of 52 mm/hr, which was twice the recorder's intensity and which fell only a short distance away (plate 3). This illustrates the fact that storm intensity sequences and rainfall hydrology parameters, like the maximum intensity for different duration, can now be evaluated for any target area, using a combination of the radar grid points.

For comparison, the rainfall of Nov. 29, 1991, was analyzed from a rain recorder and from radar grid points over this gauge. Figure 1(a, b and c) presents the storm rain segments, as well as the maximum intensities, for chosen time durations. Figure 1a shows measurements for

the rain recorder. Figure 1b shows radar measurements for the 1 km^2 of the recorder location and Figure 1c indicates radar measurements for the entire watershed area.

Figures 1a, 1b and 1c show that the maximum intensities for 30 min (I30), for example, are 38, 28 and 21 mm/hr, respectively. I30 serves not only for hydrological calculations, but also as important factor in soil erosion prediction (Wischmeier 1959). It is obvious from the differences given in the figures that watershed rain intensity spatial disposition is poorly presented by the single recorder gauge.

Radar calibration by the WPMM in the Yavne region was based on five recording rain gauges. A comparison between rain amounts for 24 hours obtained for the radar grid points and for the rain gauges is presented in Figure 2, Map 2 and Table 1. A total average storm rainfall amount of 328 mm was collected from 17 accumulating rain gauges during the November 28 to December 4, 1991 storm (Table 1). Map 2 presents the location of the gauges, as well as the differences in percentage, for each grid point, between the ground gauge measurements and the radar measurements of the storm's total rainfall. Figure 2 presents regression and correlation analysis between the daily rain depth, collected from the rain gauges and that estimated by the radar over the same locations.

From the map, figure and table it can be seen that the regional average amount and the standard deviation of the 17 stations are similar for the gauges and the corresponding radar grid points. A regression coefficient of $r^2=0.9$ and a standard deviation of 9.6 mm were obtained by the daily rain amount regression analysis. The above comparison analysis was made between a set of rain gauges with an orifice of 200 cm^2 and grid points of 1 km^2 each.

METHODOLOGY

In the second stage of the project we started to investigate the possibilities for improvement of the accuracy of the rainfall estimates by identifying the parameters causing variability in the Ze-R relationships. The Ze-R relationships depend mainly on:

1) Range from the radar, with decreasing accuracy of radar rain estimates with range.
2) Height of freezing level, with decreasing accuracy at lower freezing levels.
3) Type of rainfall, whether stratiform or convective. Different rain intensity is matched to the same echo intensity on stratiform and convective rainfall.
4) On convective rainfall, large inaccuracies are inflicted by partial radar beam filling that occurs in large horizontal gradients of rain intensity.

The WPMM methodology, described before, treats this problems. However successful application of these methodologies for items 3 and 4 above requires a good synchronization between the rain gauges and the radar, within 2 minutes. This requires digitally recording rain gauges, which we could not afford due to the very small budget.

In the 1992/93 rainy season the classification criteria of rain regimes was done in a way that, according to our understanding, would stratify the rain regimes in a meaningful way with respect to the differential intensity distributions of R and Ze, and hence also to the Ze-R relationships. One of the classification criteria is the averaged horizontal radial reflectivity gradients (Rg), which is approximation to the true horizontal reflectivity gradients. Rg, dominates the differences between the true reflectivity (Z) and the observed reflectivity (Ze), and thus the variation in the Ze-R relationships. Rg is also an approximation to the degree of convectivity of rain clouds, and hence to the drop size distribution and the absolute vertical velocity of rain drops. Figure 2 shows the Ze-R relation that were calculated from radar and gauge observations for different Rg intervals, for the range interval of 41-66 km from the Tel-Aviv airport radar. For example, it can be seen that reflectivity of 30 dB would be translated to 3.5 mm/hr for small Rg ($Rg < 2$ dB/km), but for cases of high Rg ($6 < Rg < 12$ dB/km) it would be 9 mm/hr. It can be seen that the Ze-R relations are distinctly different from each other, and the differences are ordered in agreement with changes in the classification criteria. Those trends are replicated independently for the two rainy season and for the different range interval that were analyzed.

Map 1 presents the locations of recorder rain gauges which served the calibration as well as the daily rain gauges for the control. The long axis parallel to the Mediterranean Sea covers range of 80 km from the radar to both sides; North and South. The narrow axis of 20 to 30 km from the sea to the East is due to the mountain limitation.

Figure 3 and Map 3 presents the December storm, which was the heaviest rain storm of 1992/93 season. The map and the figure present a region of about 600 km^2, which lay 20 to 45 km south of the radar location. Good correlation of 0.92 and relatively low Std. of 5% characterized the relations between the ground gauges and the radar echo interpretations.

Figure 4 and Map 4 presents the February 1992/93 storm which had low freezing level for the same area as for December 1992/93 storm. Correlation drops to 0.6 and the Std. of daily comparison between the gauges Std. the ground gauges and the radar echo was 10.8%.

The good performance of the case studies obtained for 1991/92 rainy season is mainly due to the facts that they are in relatively close ranges, high freezing level and relatively homogeneous rain regime.

Upon application of the methodology to other case studies, with lower freezing level, more variable rain types, and longer ranges from the radar, we obtained significant improvement only when using the freezing level classification. However, when trying to apply other criteria such as horizontal gradients no further improvement was achieved. We attribute it mainly to the problem of lack of synchronization. It should be noted here that testing this method on digitally rain gauge and radar from Darwin, Australia, did provide a tangible improvement.

UNITED STATES TEAM RESULTS

INTRODUCTION

Low frequency, large flood events can have substantial economic impacts on flood plain agriculture and human infrastructure. Accurate estimation of the peak runoff rate of these floods is critical for both the design of flood control structures as well as for transportation and agricultural structures. In many cases peak runoff rates are highly correlated to runoff volume and therefore accurate estimation of peak rates is valuable for runoff volumes and therefore water supply estimation. Monitoring large runoff events in semi-arid regions over a large areas is a very difficult and expensive task due to the low frequency of occurrence of such events for a given location and the difficulty of runoff measurement in ephemeral stream channels which often have mobile channel beds. Due to the short duration of convective thunderstorms typical of many arid regions, the runoff peak may have passed before being measured directly. These factors have resulted in indirect slope-area measurements of peak discharge (Dalrymple and Benson, 1967; and Chow, 1959) as the common method used to estimate peak discharge in circumstances where personnel or permanent instrumentation are not in place. Even in locations where stage gaging stations exist, indirect measurements are often used as the principal basis for extending stage-discharge ratings into the flood-stage regime when current meter measurements cannot be made (Kirby, 1987).

Indirect discharge measurements are made by locating a relatively straight section of confined river channel where post-flood analysis of flood high water marks is carried out. In this procedure (Benson and Dalrymple, 1967) erosion marks or debris lines left at peak flood stage are located on both sides of the channel. These marks are accurately surveyed to estimate a high-water surface profile for both sides of the channels. Based on the high water mark profile and channel conditions, three cross-section locations are typically selected to provide a uniform high water slope profile between the cross sections. Cross sections are then surveyed perpendicular to the flow to estimate the area of flow at peak discharge. Between the surveyed cross sections, special note is made of the channel and overbank ground material and ground cover (vegetation or other obstructions) so that hydraulic roughness values can be estimated. Slope-area computations based on the principles of conservation of matter and energy can then be carried out assuming quasi-steady state conditions at the time of peak discharge so the high-water marks from the flood crest are representative of the actual water-surface elevations and slopes (Henderson, 1966, P. 376).

However, indirect peak discharge measurements are subject to much greater error than direct runoff measurements (Potter and Walker, 1985). It is important to quantify indirect runoff measurement uncertainty in semi-arid channels as these measurements are prone to errors due to location and interpretation of post-event flood high water marks and the highly mobile alluvial channel beds during a large runoff event. When substantial channel bed scour or deposition occurs the cross-sectional channel geometry is not constant. This violates a primary assumption used in making indirect measurements (Dalrymple and Benson, 1967; Kirby, 1987). The primary objective for this part of the research was to quantify the uncertainty associated with peak flood discharge estimates obtained from post-flood, indirect methods in ephemeral regions.

This was accomplished by comparing the indirect measurements to direct stage-discharge measurement using special runoff flumes of the USDA-ARS Walnut Gulch Experimental Watershed.

THE STUDY SITE

The work was carried out in the USDA-ARS Walnut Gulch Experimental Watershed in Southeastern Arizona (see Map 5). This watershed offers unparalleled instrumentation and historical data for semi-arid hydrologic analysis (Renard et al., 1993). The watershed is especially equipped with fixed cross-section, critical depth, runoff measuring flumes which are especially designed to accurately measure sediment laden runoff typical of ephemeral semi-arid channels (see Plate 5; from Smith et al., 1982). Twelve subwatersheds equipped with these flumes, with drainage areas ranging from 2.3 to 150 km^2, provide a wide range of channel sizes and conditions (see Map 6).

Field and orthophoto map reconnaissance of the Walnut Gulch watershed was carried out to select relatively confined, straight, channel reaches which are required to make good indirect discharge measurements. A subset of channel reaches, up and downstream of the 12 recording supercritical runoff flumes, were selected as primary target locations. A field team was then assembled and put on flash flood notice so that indirect discharge measurements could be made shortly after the occurrence of runoff events during the 1993 monsoon season.

The 1993 monsoon season was very dry which limited our ability to perform indirect discharge measurements. This further illustrated the importance of the proposed research by reinforcing the point that high magnitude runoff events occur in any given location with very low frequency. Four rainfall-runoff events did occur which were utilized for this study from watersheds 9 (2 events), 10 and 6. The events were not of great magnitude but our team had to weigh the chances of getting any measurements at all during this particularly dry year. These measurements will still allow testing of the proposed methodology but uncertainty estimates for very large runoff events cannot be made without associated indirect discharge measurements. One of the primary factors that cannot be tested with the four events is the impact of channel scour or fill. Inspection of the channel beds and digging of shallow holes at the location of the indirect measurements indicated that there was very little channel bed mobilization for these four events. The location and date of the indirect discharge measurements that were made are summarized in Table 1.

THE INDIRECT DISCHARGE MEASUREMENTS

At each of the four locations noted in Table 1 the field team initially examined the channel reaches for evidence of high-water marks. Benchmarks on each of the nearby flumes were assigned arbitrary coordinates and a total surveying station was used to establish survey control for each of the channel reaches where the indirect measurements were made. In the next phase of the survey, X, Y, and Z coordinates were computed for a series of high-water marks on both the left and right bank of the channel to define the areal extent of the flood at peak runoff stage.

This is illustrated in Figure 5 for the Aug. 19, 1993 event downstream of Flume 9. A photograph looking downstream of the indirect discharge measurement reach for this event is presented in Plate 6a. The high-water mark elevations were then plotted as a function of distance parallel to the primary flow direction to estimate the water surface profile at peak stage. The high-water profiles for both banks are illustrated in Figure 6 for the Aug. 19, 1993 event downstream of Flume 9 and in Figure 7 for the Aug. 31, 1993 event downstream of Flume 6. The importance of these profiles cannot be underestimated as they must be plotted in the field and are used to select the location of the channel cross-section surveys. This is required so that relatively uniform water surface slope exists between the cross sections so that theoretical assumptions for the computation of peak discharge estimates are not violated.

The two surface profile cases illustrated in Figure 6 and 7 represent the best and worst case of the four indirect measurements made for estimating high-water mark profile slope. In the best case (Figure 7 - downstream of flume 6) the profiles are very smooth and quite uniform with some divergence at the upstream end of the reach. However, selection of the cross section locations and assigning water surface elevations at these cross sections using the midpoint between left and right bank elevations is quite straight forward. In contrast to the good profiles illustrated in Figure 7, those in Figure 6 contain erratic fluctuations, particularly on the right bank profile. This is attributed to the displacement of the high-water marks due to bank collapse that is illustrated in Plate 6b. Greater emphasis was therefore placed on the left bank profile for estimating the water profile slope. The profile on the left bank is far better than that on the right but a good deal of judgement is still required to estimate the slopes. The subjectivity in selection of high-water mark slope estimates and its subsequent impact on peak discharge estimates is treated in more detail in the following section which treats some of the uncertainties involved in making indirect discharge measurements.

Cross sectional surveys were then performed while making detailed notes of the bed material and surface cover which have direct bearing on the estimation of the appropriate values of hydraulic roughness. Plots of all the high-water mark plan views, profiles and cross sections for each of the four events are contained in Appendix A. The "best" estimates of the Manning's hydraulic roughness coefficient (n) for each of the indirect measurements are contained in Table 3. Also included in the table are typical ranges of values of (n) for the type of channel conditions that were present. As in the case of slope estimation, subjective judgement is required in the process of assigning hydraulic roughness values which adds to the uncertainty of peak discharge estimation via indirect discharge measurements. This will be examined further in the following section.

Computer programs were then developed to reduce the survey data and determine the necessary geometric properties for slope-area flow computations such as cross sectional area, wetted perimeter and hydraulic radius. This data was coupled with the estimates of water surface slope and hydraulic roughness to compute estimates of peak discharge as described in Dalrymple and Benson, 1967). The observed peak stage (water depth) measurements from the fixed cross section critical depth Walnut Gulch flumes were used with the applicable rating tables to compute observed peak discharge. The peak runoff estimates from both the indirect and flume measurements as well as percentage errors of the indirect measurements are contained in Table

4. The results are summarized graphically in Figure 8. The table and the figures indicate that by in large, the indirect peak discharge estimates agreed very well with those observed by the Walnut Gulch flumes. This is probably the result of several factors. First, the personnel making the measurements are highly experienced and very familiar with the hydraulic and hydrologic conditions in Walnut Gulch. Secondly, as noted above, the events that occurred and where measured in the dry summer of 1993 were relatively small with little or no evidence of significant channel bed scour or bed mobilization.

INDIRECT MEASUREMENT UNCERTAINTY ANALYSIS

As noted above, a number of subjective decisions must be made to compute indirect peak discharge estimates. Surface water slopes obtained from high water marks are subject to uncertainty due to wave surge and small contractions and expansions in cross sectional flow area. In addition, the hydraulic roughness is also subject to considerable interpretation for a given reach. Because the observed peak discharge measurements were used as a basis of comparison for the indirect peak discharge measurements their relative accuracy must also be assessed.

This assessment was carried out by Smith et al. (1982) via a special set of discharge measurements made at flume 6. To make these measurements a bridge was constructed over the flume which allowed the installation of a several sonic depth measurement devices and a velocity meter that could swiftly traverse the flume and digitally record both depth and velocity to compute discharge. These measurements were compared to the depth-discharge ratings developed from scale model studies conducted in laboratory flumes. From these measurements it was determined that the laboratory ratings tended to slightly underestimate the discharge by roughly three percent at a discharge of 20 m^3/s and increasing to an approximate four percent underestimation at 30 m^3/s. Assuming that the metered discharge measurements are correct, a conservative estimate of the flume discharge error of plus or minus four percent was made. This implies that if indirect peak discharge measurements are within four percent of the observed flume discharge they will not be considered different. The four percent error envelope associated with the stage-discharge rating is displayed in the subsequent figures when considering the uncertainty associated with estimation of water surface slope and the hydraulic roughness.

To assess the uncertainty associated with the subjective estimation of slope and hydraulic roughness the peak discharge calculations were repeated for reasonable upper and lower limits of these values. For roughness values the observed "best" estimates were increased and decreased by 20 percent. A 20 percent deviation was selected based on the range of visual estimates made by several staff of the Southwest Watershed Research Center of the indirect study reaches. In addition, this range of deviation is typically within the range of published roughness values for the type of channel and overbank conditions present (Chow, 1959; Woolhiser et al., 1990). The resulting impact of the 20 percent variation in the roughness values is illustrated in Figure 9. As illustrated in this figure the variation in roughness can have a substantial impact on the computed peak discharge.

To assess the uncertainty arising from variation in water surface profile slope the left and right bank high-water profiles for each indirect measurement were examined (Figures 6 and 7; also see Appendix A). For each case the left and right bank profiles were interpreted in such a way as to estimate maximum and minimum slopes where as the initial analysis utilized interpreted "average" slopes. Selecting different slopes implies different water surface elevations at the indirect measurement cross sections. Therefore the cross-sectional flow area, wetted perimeter, and hydraulic radius are also impacted by this change. The slope extremes, coupled with the associated changes in cross section properties were used in the indirect peak discharge computations and the range of variation in peak discharge around the those obtained from the base (average) slope values is illustrated in Figure 10. The range of variation in peak discharge due to using slope extremes is roughly comparable to the changes induced by a 20 percent variations in roughness and can impart large percentage changes in computed peak discharge.

The envelope of variation in peak discharge due to simultaneous variation of roughness and slope extremes was then examined. In one case the minimum slope was coupled with the 20 percent increase in roughness and at the other extreme the maximum slope was coupled with the case of a 20 percent decrease in roughness. These combinations produced the largest range in variation for the two factors. The results are illustrated in Figure 11. The combined effect on the indirect peak discharge computations was generally more pronounced for the case of maximum slope and a decrease in roughness resulting in large over estimates.

The envelopes of variation in indirect peak discharge computation illustrated in Figures 9 through 11 represent realistic estimates of the range of uncertainty that might be expected. Values of the average absolute difference in cms (m^3/s) and average of absolute percentage differences over the four events are contained in Table 5. Greater uncertainty in indirect discharge estimation can be expected for larger events in which channel scour or fill may occur. Kirby (1987) concluded that scour and the resultant inaccurate measurement of channel cross sections dominated the errors associated with indirect discharge measurements and "as long as scour uncertainty exists, improvements in measuring other factors seem to be of limited benefit". Unfortunately, as stated earlier, no large flood events occurred during the course of this study where the impacts of scour or fill on measurement accuracy might be assessed. In the future our team will attempt to make indirect discharge measurements for such events should they occur.

The uncertainty of the indirect discharge measurements made in this study as compared to the observed peaks from the supercritical flumes is small. Rainfall-runoff model predictions are not likely to exceed the accuracy of the "good" indirect discharge estimates made as part of this study. Detailed rainfall-runoff modeling of the events for which indirect measurements were made in this study was precluded by the decrease in funding and reflected in the revised work plan. Future efforts will be directed to carry out this modeling. However, some indication of the ability of rainfall-runoff models to predict peak discharge can be obtained from Goodrich (1991) on the nearby Walnut Gulch subwatershed 11. This study utilized high spatial resolution rainfall data from the extensive raingage network in the watershed. If this rainfall data is considered a surrogate for data that might be obtained from radar data, the ability of a system

to collect outlier flood peak data from radar-rainfall data input to a rainfall-runoff model can be examined.

For Walnut Gulch Watershed 11 (6.31 km^2) the KINEROS rainfall-runoff model (Woolhiser et al., 1990) was applied for 10 events which varied over a range of size using rainfall input from 10 recording raingages. The model parameters were not calibrated to observed data and the peak discharge was estimated for the ten events. Using the model computed peak discharge rates and those observed at the flume the same values as those presented in Table 5 were computed. The average absolute difference in peak rate (average of abs(Qp_{model} -$Qp_{observed}$) was 3.18 m^3/s) and the average of the absolute percentage differences over the ten events was 51.25%. When these numbers are compared to those in Table 5 for several of the cases where roughness, slope or a combination of the two are varied within reasonable ranges it is evident that a runoff model with high resolution rainfall data may be able to predict peak runoff rates with comparable accuracy to indirect discharge measurements in an average sense as indicated by the measures in Table 5. If flood events occur with substantial channel scour or fill, the uncertainty of the indirect discharge measurements is likely to increase and the radar-rainfall-runoff modeling approach may become more viable. This conclusion must, of course be made with extreme caution, as the sample size of indirect measurements is small and the model results are from an adjacent basin. A larger data set and more extensive modeling analysis will be required to draw any strong conclusions.

EVALUATION OF THE RESEARCH ACHIEVEMENTS

A methodology for rainfall measurements with radar for hydrological applications was developed and evaluated. The overall accuracy was impressive. However, significant errors still remain, and leave still much room for further work. These calculated differences between the radar and gauge measurements may result from:

a. Errors in matching the radar grid points with the rain gauge in time and space;
b. Inaccuracies in the Ze-R relationship;
c. Variations due to a large difference in the measured rain area; and,
d. Errors in gauge readings between the radar and the rain gauge (mostly the result of different reading times).

At this stage in the research we cannot quantify the relative contribution of the different sources of errors. However, timing and placement problems are canceled out through integration over a catchment area and over time.

In addition, a comparison of indirect peak discharge measurements to peak runoff estimates from supercritical flumes was carried out in ephemeral channels of a semi-arid experimental watershed. Four measurements were made of floods that were small to medium in magnitude. For these events indirect measurements compared very well with flume observations. Uncertainty analysis for the impacts of roughness and water slope variations on indirect peak estimates indicated that substantial variation in peak discharge can result from realistic variations

in roughness and slope as interpreted from the field data. The uncertainty of indirect peak discharge estimation was then compared to rainfall-runoff modeling results from a nearby subwatershed. The comparison indicated that high spatial resolution rainfall data and a distributed runoff model may be able to predict peak runoff rates with comparable accuracy to indirect measurements. However, a larger data set and more extensive modeling analysis will be required to draw any strong conclusions. If this conclusion does hold, the possibility exists to develop an arid lands water resources monitoring system for outlier events on ungaged watersheds using radar rainfall measurements.

In summary, two important components of a system to collect outlier flood peak estimates have been evaluated. Although the two research components were developed in separate locations, the results will build the foundation for testing the system within the Walnut Gulch watershed when NEXRAD radar data becomes available using the Window Probability Matching Method algorithms for radar-rainfall inputs into a distributed rainfall-runoff model.

Acknowledgments

The authors gratefully acknowledge the support of the International Arid Lands Consortium and the USDA-Forest Service. We would also like to thank Electrical-Mechanical-Services, a subsidiary of Mekoroth, the Israeli national water company, for the radar data. The authors are also grateful to the Israel Meteorology Service for using their rain gauge data. This research was supported in part by a grant from the United States -Israel (Binational) Agricultural Research and Development Fund (BARD) and in part by the Israeli Jewish National Fund. In addition we would like to thank the staff of the Southwest Watershed Research Center for their support and field assistance.

REFERENCES

Battan L. J., 1973: Radar observations of the Atmosphere. The University of Chicago Press, 324 p.

Benson, M. A., and Dalrymple, T., 1967. General field and office procedures for indirect discharge measurements. Tech. Water-Res. Invest. U.S. Geological Survey, Book 3, Chapter A1, Application of Hydraulics, U.S. Gov. Printing Off., Wash. D.C., 30 pp.

Chow, V. T., 1959. Open-Channel Hydraulics, McGraw-Hill Book Co., N.Y., N.Y., p. 148-150.

Dalrymple, T., and M. A. Benson, 1967. Measurement of peak discharge by the slope-area method. Tech. Water-Res. Invest. U.S. Geological Survey, Book 3, Chapter, A2, Application of Hydraulics, U.S. Gov. Printing Off., Wash. D.C., 12 pp.

Donaldson R. J., 1964: A demonstration of antenna beam errors in radar reflectivity patterns. J. Appl. Meteror., 3, 611-623.

Goodrich, D. C., 1991. Basin scale and runoff model complexity. Univ. of Arizona, Dept. of Hydrology and Water Resour. Tech. Rep. No. HWR 91-010, June., 361 p.

Henderson, F. M., 1966. Open Channel Flow, Macmillan, New York, N.Y., 680 pp.

Joss J., J. C. Thams and A. Waldvogel, 1968: The accuracy of daily rainfall measurements by radar. 13th Radar Meteorology Conf., Montreal, 448-451.

Joss J., K. Schram, J. C. Thams and A. Waldvogel, 1970: On the quantitative determination of precipitation by radar. Scientific Communication No. 63, Research Dept. of the Federal Commission on the Study of Hail Formation and Hail Suppression, Ticinese Observatory of the Swiss Central Meteorological Institute, Federal Institute of Technology, Zurich, 38 pp.

Kirby, W. H., 1987: Linear error analysis of slope-area discharge determinations. J. Hydrology, 96:125-138.

Klazura G. E., 1981: Differences between some radar-rainfall estimation procedures in a high rain rate gradient storm. J. Appl. Meteor., 20, 1376-1380.

Konrad T. G., 1978: Statistical models of summertime rainshowers derived from fine-scale radar observations. J. Appl. Meteor 17, 171-188.

Marshall J. S. and W. McK Palmer, 1948: The distribution of raindrops with size. J. Meteor., 5, 165-166.

Morin, J. and Sharon, D., 1993. Rainfall intensity analysis as a tool for water resources planning. Geographical Scripts ITH (Zurich), 53: pp 52-59.

Potter, K. W., and Walker, J. F., 1985. An empirical study of flood measurement error. Water Resources Research, 21(3):403-406.

Renard, K. G., L. J. Lane, J. R. Simanton, W. E. Emmerich, J. J. Stone, M. A. Weltz, D. C. Goodrich, D. S. Yakowitz, Agricultural impacts in an arid environment: Walnut Gulch case study. Hydrological Science and Technology, 9(1-4):145-190, 1993.

Rogers R. R., 1971: The effect of variable target reflectivity on weather radar measurements. Quart. J. of Roy. Met. Soc., 97, 154-167.

Rosenfeld D., D. Atlas, D. B. Wolff and E. Amitai, 1992: Beamwidth effects on Z-R relations and area-integrated rainfall. J. Appl. Meteor., 31, 454-464.

Rosenfeld, D., Amitai, E. and Wolff, D.B., 1994b. Classification of rain regimes by the 3-dimensional properties of reflectivity fields. J. Appl. Meteor., (Accepted).

Rosenfeld, D., Amitai, E. and Wolff, D.B., 1994c. Improved accuracy of radar WPMM estimated rainfall upon application of objective classification criteria. J. Appl. Meteor., (Accepted).

Rosenfeld, D., Wolff, D.B. and Amitai, E., 1994a. The window probability matching method for rainfall measurements with radar. J. Appl. Meteor., (Accepted).

Smith, R. E., D. L. Chery, Jr., K. G. Renard, and W. R. Gwinn, 1982. Supercritical flow flumes for measuring sediment-laden flow. USDA-ARS Tech. Bull. No. 1655, 70 p.

Stout G. E. and E/ A. Mueller, 1968: Survey of relationships between rainfall rates and radar reflectivity in the measurement of precipitation. J. Appl. Meteor., 7, 465-473.

Szoke E. J., E. J. Zipser and D. P. Jorgenson, 1986: A radar study of convective cells in mesoscale systems in GATE. Part I: Vertical profile statistics and comparison with hurricanes. J. Atmos. Sci., 43, 182-197.

Wilson J. W. and E. A. Brandes, 1979: Radar measurement of rainfall. Bull. Amer. Meteor. Soc., 60, 1048-1058.

Wischmeier, W.H., 1959. A rainfall erosion index for a Universal Soil Erosion Equation. Soil Sci. Soc. Am. Proc. 21: pp 246-249.

Woolhiser, D. A., Smith, R.E., and Goodrich, D.C., 1990. KINEROS, A kinematic runoff and erosion model: documentation and user manual. U.S. Department of Agriculture, ARS, ARS-77, 130 pp.

Zawadzki I. I., 1973: Statistical properties of precipitation patterns. J. Appl. Meteor., 12, 459-472.

Plate & Figure Captions:

Plate 1: Distribution of 24 hr. radar rain depth [mm] for area of 20x20 km (Nov. 29, 1991).

Plate 2: Distribution of 24 hr. radar rain depth [mm] for Yavne watershed (Nov. 29, 1991).

Plate 3: Five minutes radar rain intensity [mm/hr] for Nov. 29, 1991, 19:08-19:13

Plate 4: Five minutes radar rain intensity [mm/hr] for Nov. 29, 1991, 19:13-19:18

Fig. 1: Recording rain gauge and radar estimated rain intensity for 24 hr. starting 8AM LST, Nov. 29, 1991.

1a. Yavne rain recorder.

1b. Yavne 1 km^2 radar grid point.

1c. Yavne watershed averaged radar grid points.

Fig. 2: Daily rain depth regression between rain gauges and radar estimation over the gauges for Nov. 28, 1991 to Dec. 2, 1991.

Fig. 3: Regression between daily rain gauges and radar estimated rainfoll for the storm of 13-17 December 1992.

Fig. 4: Regression between daily rain gauges and radar estimated rainfall for the storm of 8-13 February 1993.

Map 1: The distribution of daily rain gauges locations in Israel.

Map 2: Rain depth differences in percentage for 20x20 km area for Nov. 28, 1991 to Dec. 4, 1991 rainstorm. Average rain depth: Recorder - 328 mm ; Radar- 321 mm.

Map 3: Rain depth differences in percentage for X 120-146, Y 116-140, for the storm of 13-17 December 1992.

Map 4: Rain depth differences in percentage for X 120-146, Y 116-140, for the storm of 8-13 February 1993.

Table 1: Differences between rain gauges and estimated radar rain depth for Nov. 28, 1991 - Dec. 4, 1991 rainstorm.

Plate and Figure Captions: (continued)

Plate 5: Photograph of Walnut Gulch Supercritical Runoff Flume 1.

Plate 6a: Photograph looking downstream of the indirect measurement channel reach for the Aug. 19, 1993 event downstream of flume 9.

Plate 6b: Photograph of bank collapse on the right bank of the indirect measurement channel reach for the Aug. 19, 1993 event downstream of flume 9.

Map 5: USDA-ARS Walnut Gulch Experimental Watershed location map.

Map 6: Primary subwatersheds of the Walnut Gulch Experimental Watershed.

Fig. 5: Plan view of high-water marks downstream of flume 9 (flood of Aug. 19, 1993).

Fig. 6: High-water mark surface water profile on both banks downstream of flume 9 (flood of Aug. 19, 1993).

Fig. 7: High-water mark surface water profile on both banks downstream of flume 6 (flood of Aug. 31, 1993).

Fig. 8: a) Indirect vs observed peak runoff rates, b) Percent difference in indirect vs observed peak runoff rates.

Fig. 9: Uncertainty range in indirect peak runoff estimates from a -/+ 20% variation in Manning's hydraulic roughness (n).

Fig. 10: Uncertainty range in indirect peak runoff estimates from a minimum and maximum water surface slope variation.

Fig. 11: Uncertainty range in indirect peak runoff estimates from a -/+ 20% variation in Manning's hydraulic roughness (n) coupled with minimum and maximum water surface slope combinations.

Table 2: Date and location of indirect discharge measurements

Table 3: Manning's hydraulic roughness estimate for each cross section of each indirect measurement and typical published ranges of hydraulic roughness for the material typical of the cross sections.

Table 4: Summary of observed and indirect peak discharge measurements (Qp)

Table 5: Summary Statistics of Variation in Indirect Peak Discharge Due to Variation in Hydraulic Roughness, Slope, and Combinations of Roughness and Slope

Table 1: Differences between rain gauges and estimated radar rain depth for Nov. 28, 1991 - Dec. 4, 1991 rainstorm.

STATION NAME	*LONGITUDE (km)	*LATITUDE (km)	RAINGAUGE (mm)	RADAR (mm)	GAUGE-RADAR
Havazelet	132	142	410	398	12
Netaim	129	150	247	258	-11
Eqron	134	138	311	329	-18
Brorim	129	130	293	338	-45
Palmahim	122	149	288	293	-5
Gan Shlomo	131	142	411	398	13
Bnei Darom	121	136	302	320	-18
Hafez Haim	131	133	335	287	48
Kfar Bilu	133	142	386	374	12
Nir Galim	120	137	304	314	-10
Ramle Nesher	140	147	319	287	32
Givat Brener	131	141	408	400	8
Nezer Sireni	133	148	313	283	30
Bet Hilkia	132	133	295	273	22
Hazor	123	131	306	275	32
Yavne-Kvutza	123	136	342	314	29
Hazor-Ashdod	125	130	308	313	-5
Average (mm)			**328**	**321**	**7.6**
Std. (mm)			**47**	**45**	**22.9**
CV%					**22.9/328 = 7%**

*Israel grid coordinates

DISTRIBUTION OF DAILY RAINGAUGE LOCATIONS ACROSS ISRAEL

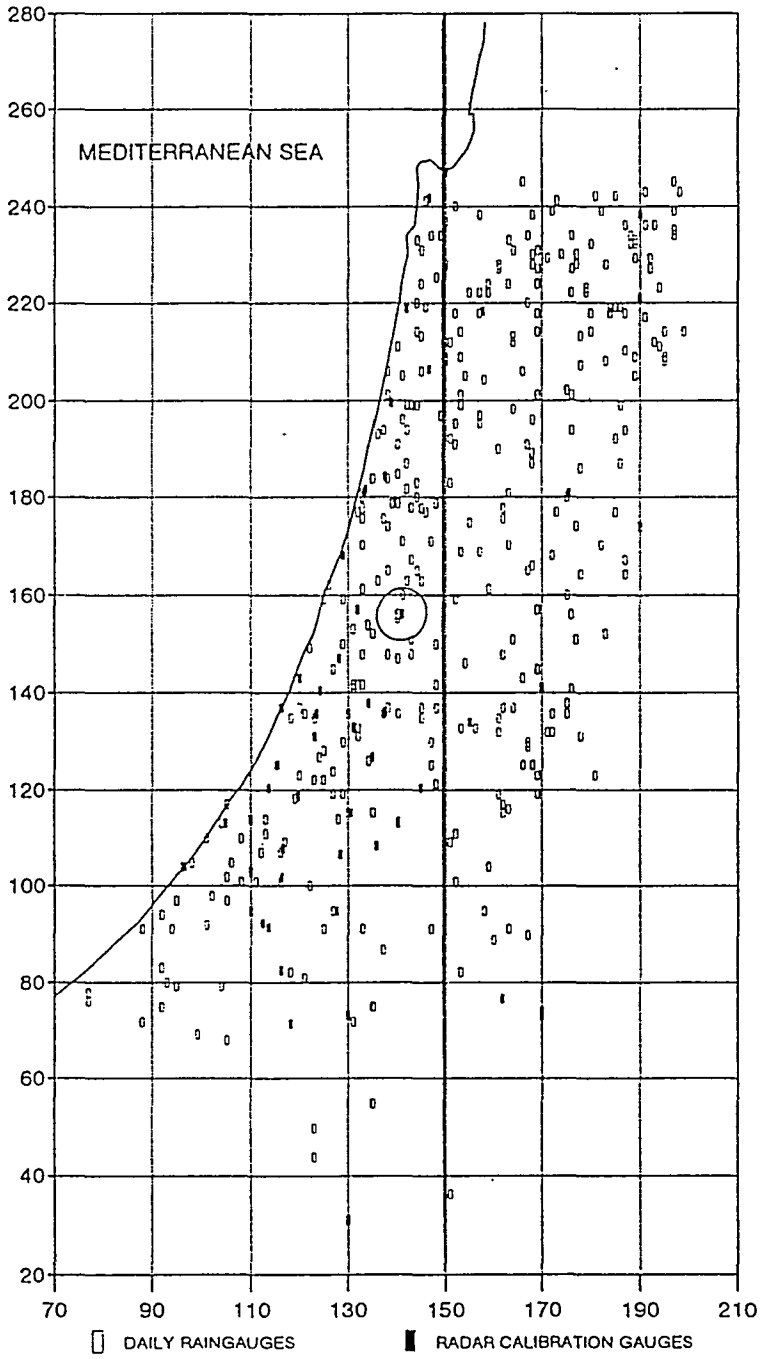

RADAR CALIBRATION STATIONS

NAME	X	Y
HAIFA	150	247
K.GALIM	147	242
M.MICHAEL	142	219
GALED	158	218
GAN SHMUEL	147	207
HOFIT	139	199
TEL ITZAK	138	185
GAASH	134	182
SHCHEM	176	181
SHFAYIM	133	181
SDE-DOV	129	168
B.DAGAN	132	157
RADAR	141	156
AYANOT	128	147
PALMACHIM	120	143
ATARO.JER	170	142
B.ZAKAI	124	141
EKRON	134	138
ASHDOD	116	137
YESODOT	137	136
YAVNE	123	136
B.MEIR	155	134
HAFE.HAIM	131	133
HAZOR	123	131
K.MENAHEM	135	127
NITZANIM	115	125
G.YESHAYA	145	120
SILVER	114	120
NEGBA	120	119
GAT	131	115
B.GOVRIN	140	113
ZIKIM	105	113
LACISH	136	108
BROR HAYIL	117	108
AHUZAM	128	107
GAZA	97	104
DOROT	116	102
B.KAMA	128	95
B.HAGDI	112	93
DVIR	113	92
GILAT	116	83
TEL ARAD	162	77
ARAD	170	74
S.SHAKED	118	72

Fig.1 RECORDING RAIN GAUGE AND RADAR ESTIMATED RAIN INTENSITY FOR 24 hr. (Nov. 29-30,1991)

1a. Yavne rain recorder

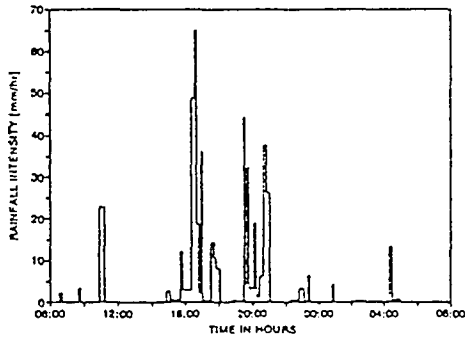

MAXIMUM INTENSITIES FOR CONTINOUS CHOSEN TIME DURATION:

DURATION(min)	INTENSITY(mm/hr)
10	62
15	57
30	38
60	23
120	14
150	13
180	11

1b. Yavne 1 sq. Km radar grid point

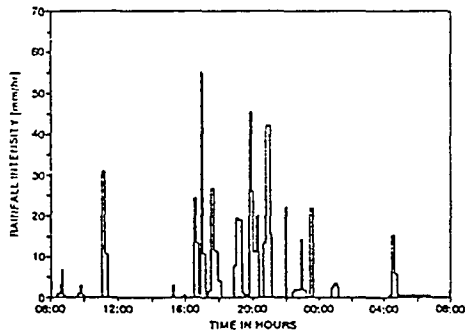

DURATION(min)	INTENSITY(mm/hr)
10	52
15	39
30	28
60	19
120	17
150	14
180	12

1c. Yavne watershed averaged radar grid points

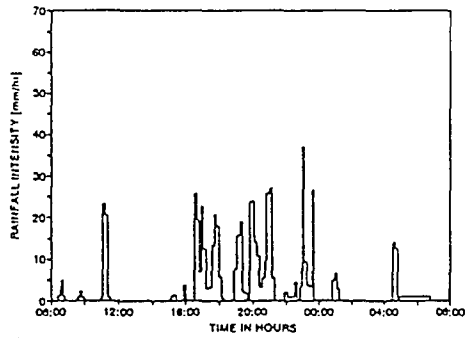

DURATION(min)	INTENSITY(mm/hr)
10	33
15	27
30	21
60	14
120	13
150	12
180	10

PIC. 1 RADAR RAIN DEPTH FOR NOV. 29, 1991
DISTRIBUTION FOR 20x20 km

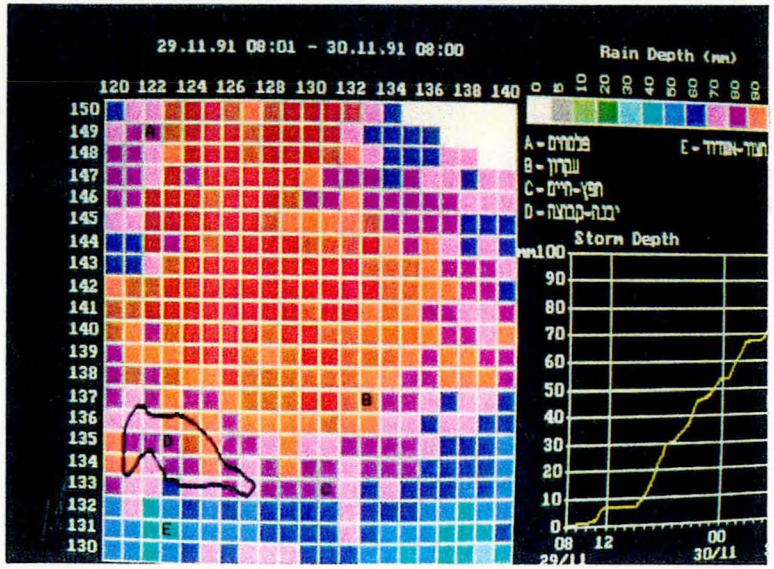

PIC. 2 RADAR RAIN DEPTH FOR NOV. 29, 1991
DISTRIBUTION FOR YAVNE WATERSHED

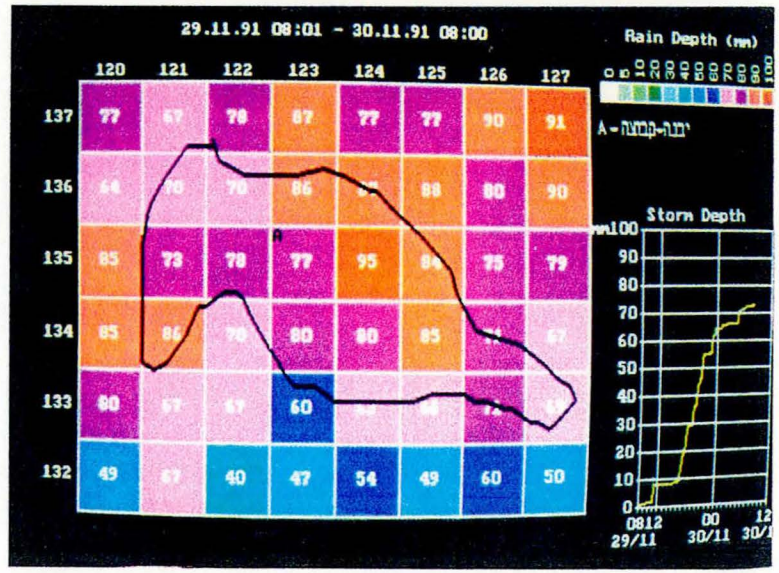

PIC. 3 RADAR RAIN INTENSITY FOR 5 min
FOR NOV. 29, 1991 19:08-19:13

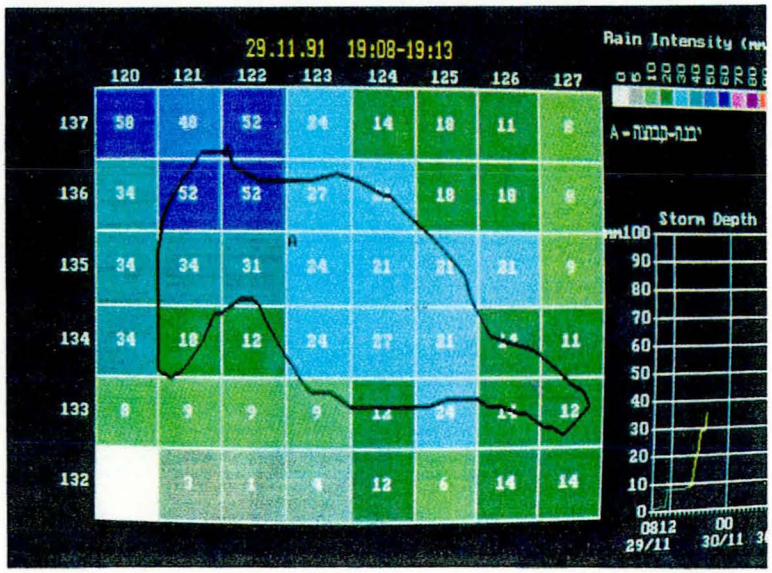

PIC. 4 RADAR RAIN INTENSITY FOR 5 min
FOR NOV. 29, 1991 19:13-19:18

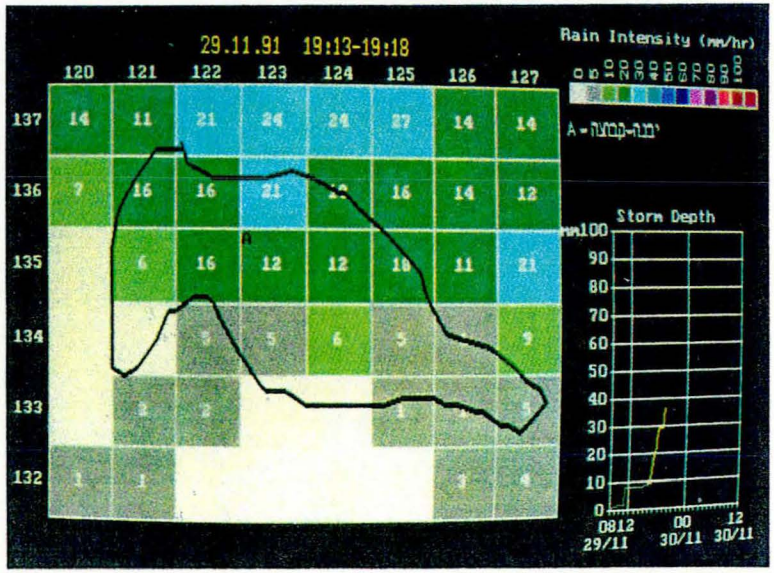

MAP- 2: RAIN DEPTH DIFFERENCES IN PERCENTAGE

FOR 20x20 km. AREA (Nov.28 to Dec.2,1991 Rain Storm)

Average rain depth: Recorder-328 mm. Radar-321 mm.

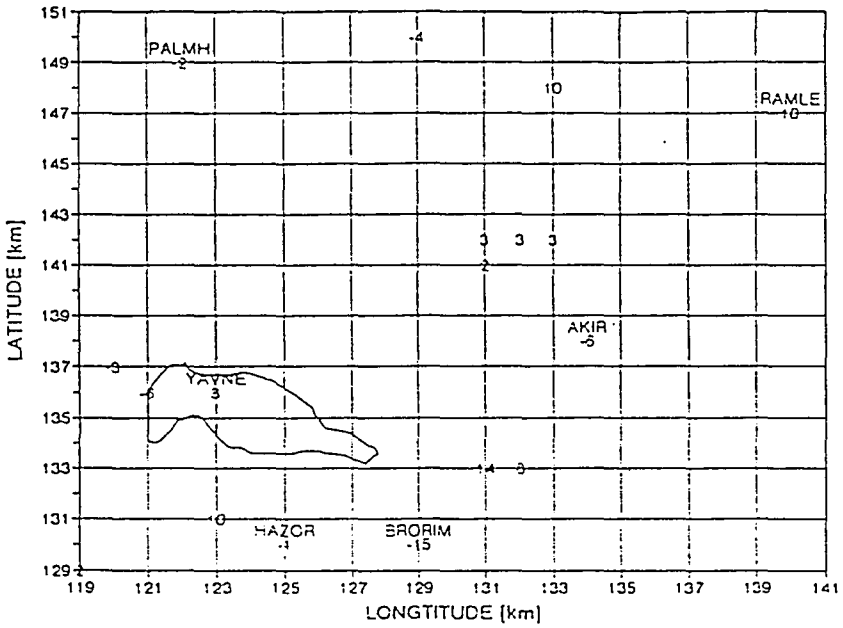

STD. Recorder- 47mm RADAR- 45mm

STD. DIFFERENCES 7% (23 mm.)

FIG. 2: DAILY RAIFALL DEPTH REGRESSION BETWEEN

RADAR ESTIMATION OVER THE GAUGES (Nov.28 to Dec.2 1991)

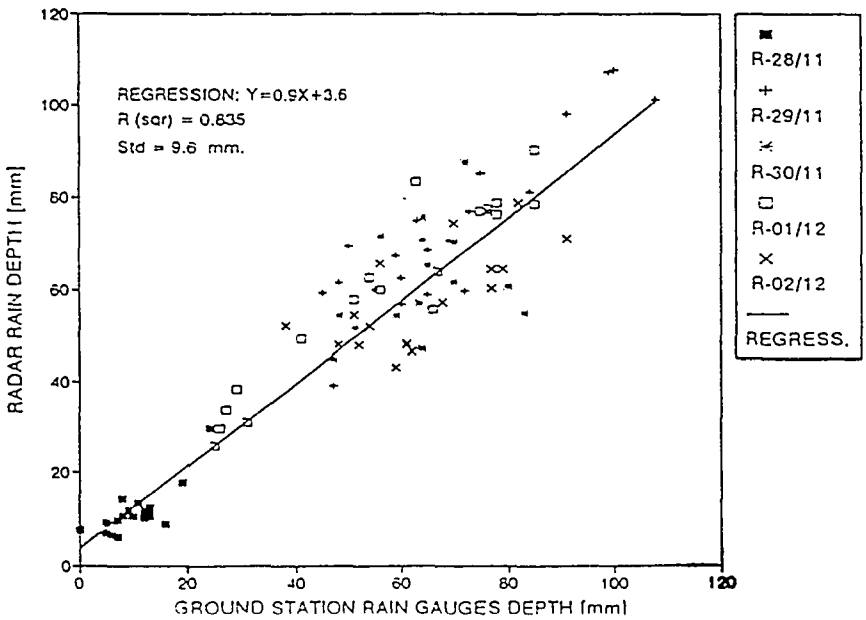

Map 3:

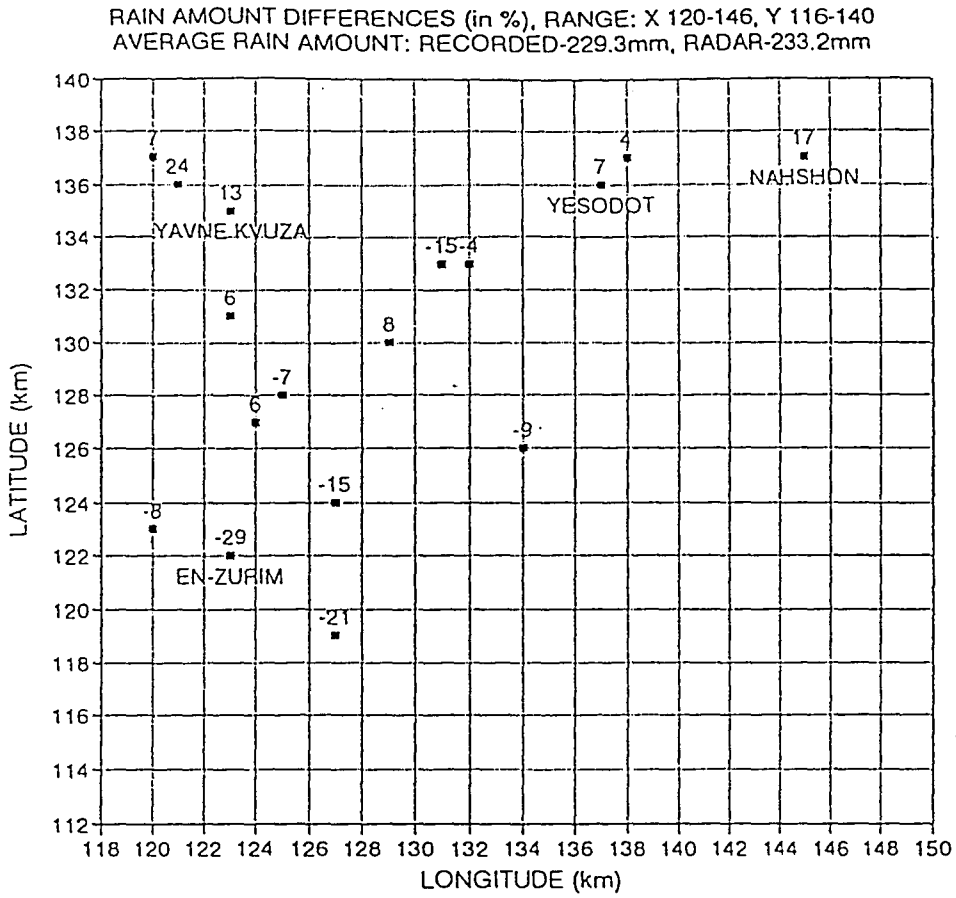

Figure 3:

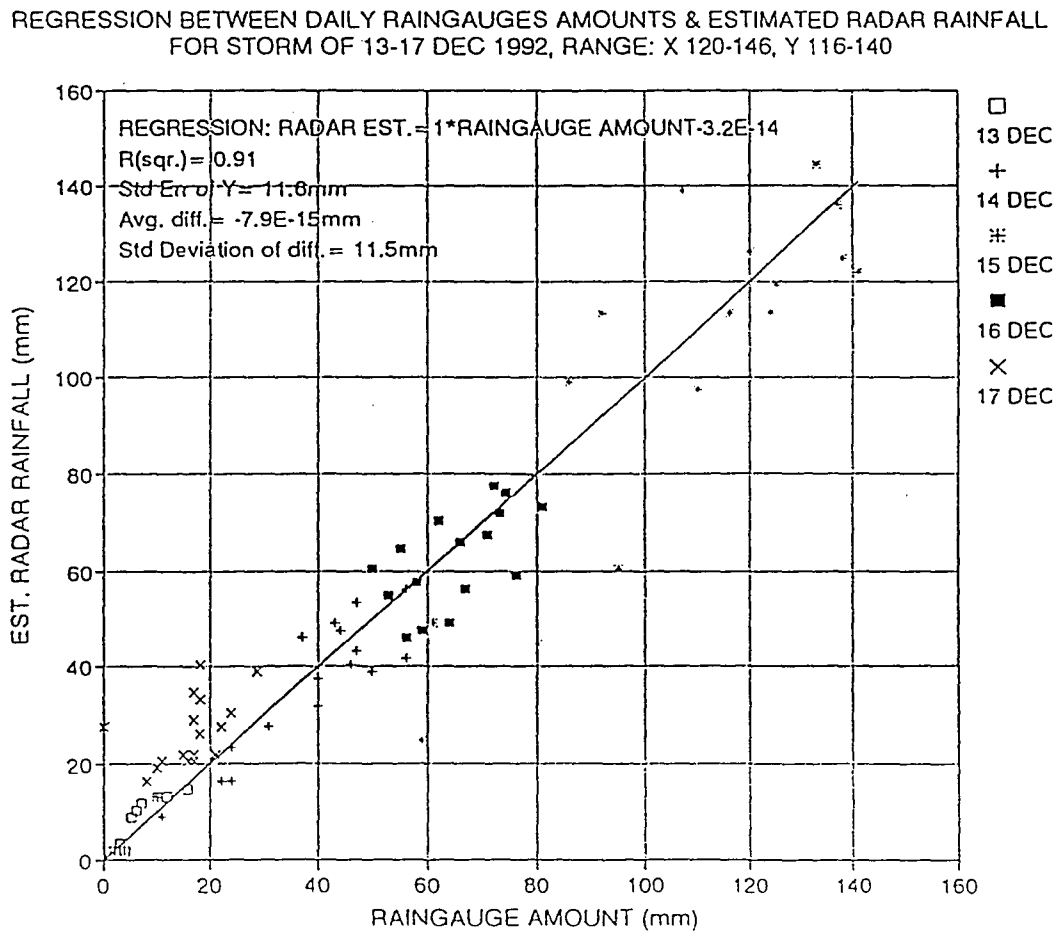
REGRESSION BETWEEN DAILY RAINGAUGES AMOUNTS & ESTIMATED RADAR RAINFALL
FOR STORM OF 13-17 DEC 1992, RANGE: X 120-146, Y 116-140
REGRESSION: RADAR EST.= 1*RAINGAUGE AMOUNT-3.2E-14
R(sqr.)= 0.91
Std Error of Y= 11.6mm
Avg. diff.= -7.9E-15mm
Std Deviation of diff.= 11.5mm
EST. RADAR RAINFALL (mm)
RAINGAUGE AMOUNT (mm)
13 DEC
14 DEC
15 DEC
16 DEC
17 DEC

Map 4:

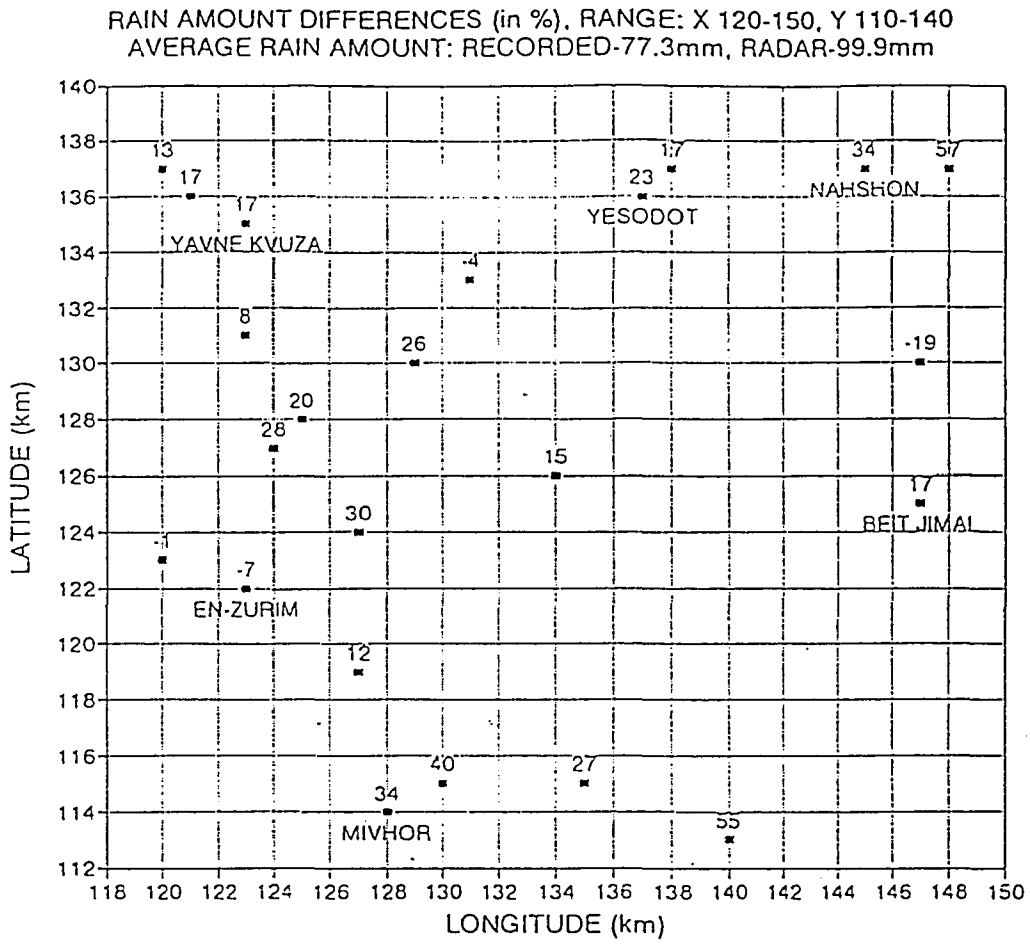

Figure 4:

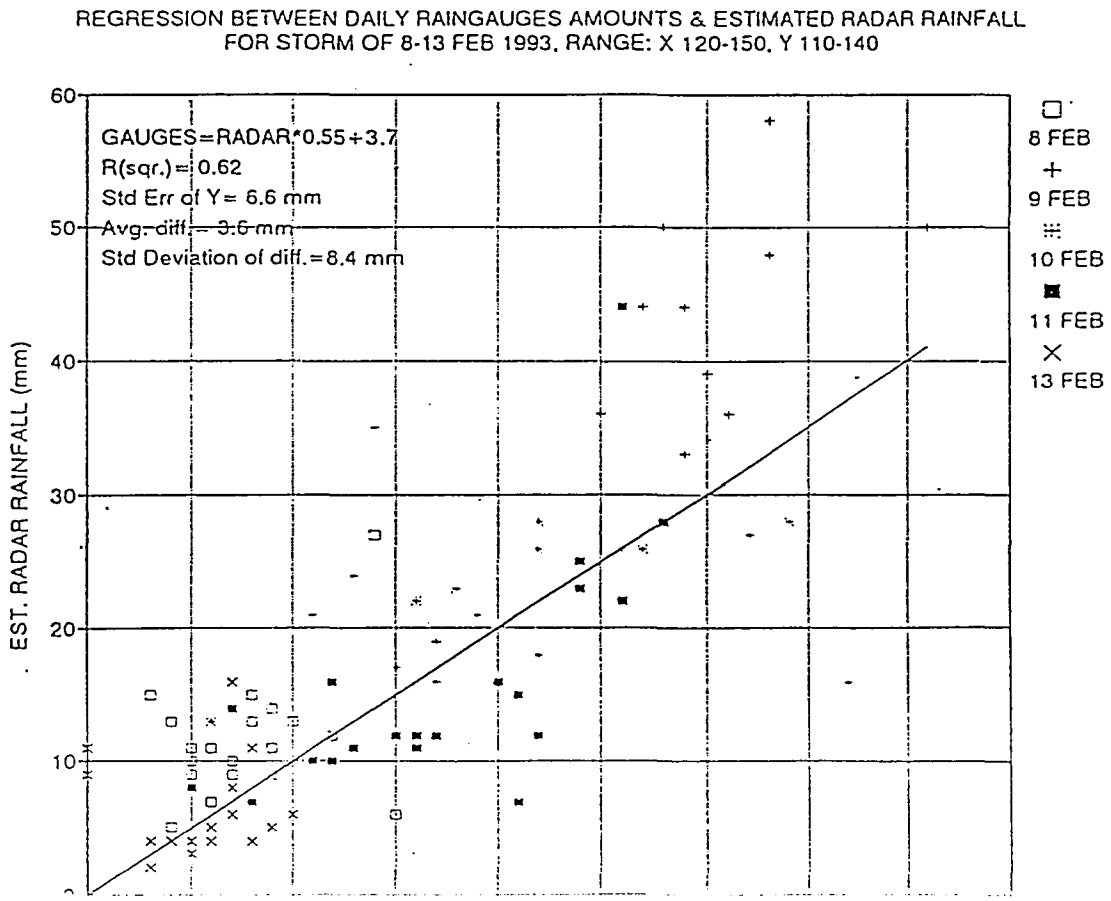

Map 5

LOCATION MAP
USDA-ARS WALNUT GULCH
EXPERIMENTAL WATERSHED

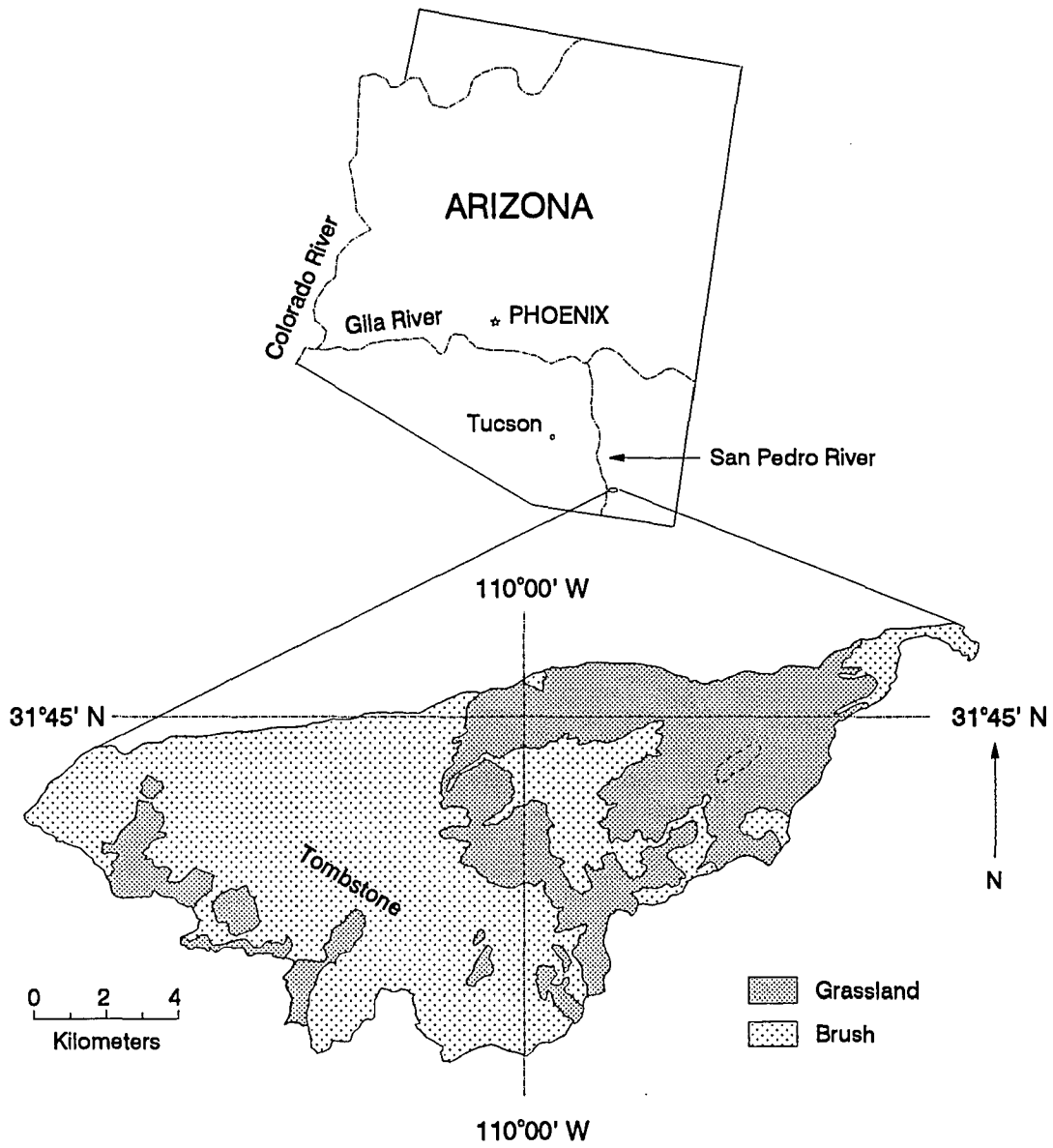

Map 6

USDA-ARS WALNUT GULCH EXPERIMENTAL WATERSHED RUNOFF FLUME AND SUBWATERSHED LOCATIONS

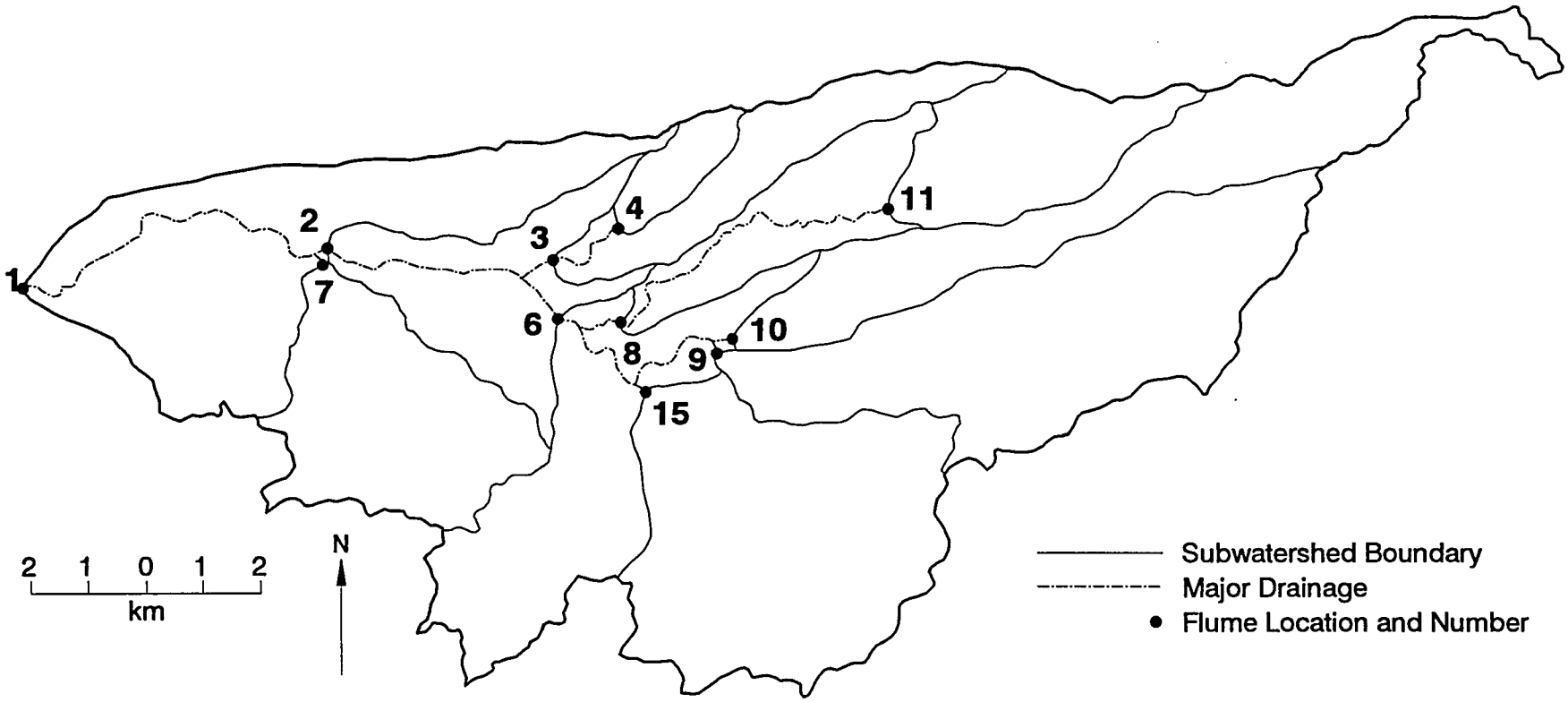

Plate 5: Photograph of Walnut Gulch Supercritical Runoff Flume 1.

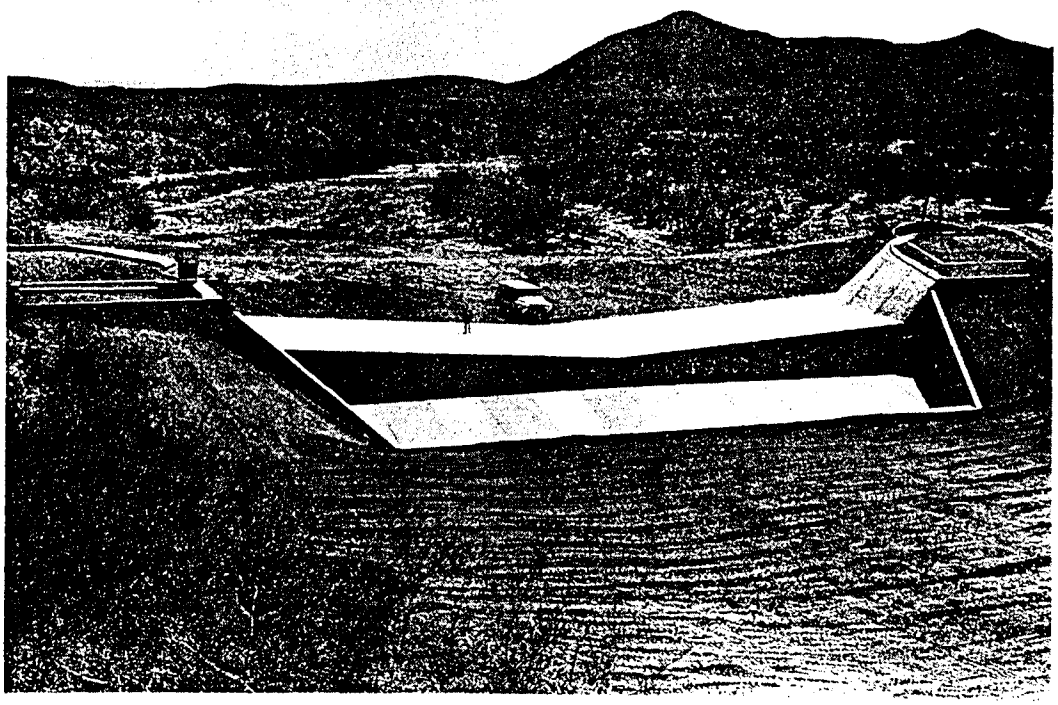

Figure 5

PLAN VIEW OF HIGH–WATER MARKS DOWNSTREAM FLUME 9
(FLOOD OF 19 AUGUST 1993)

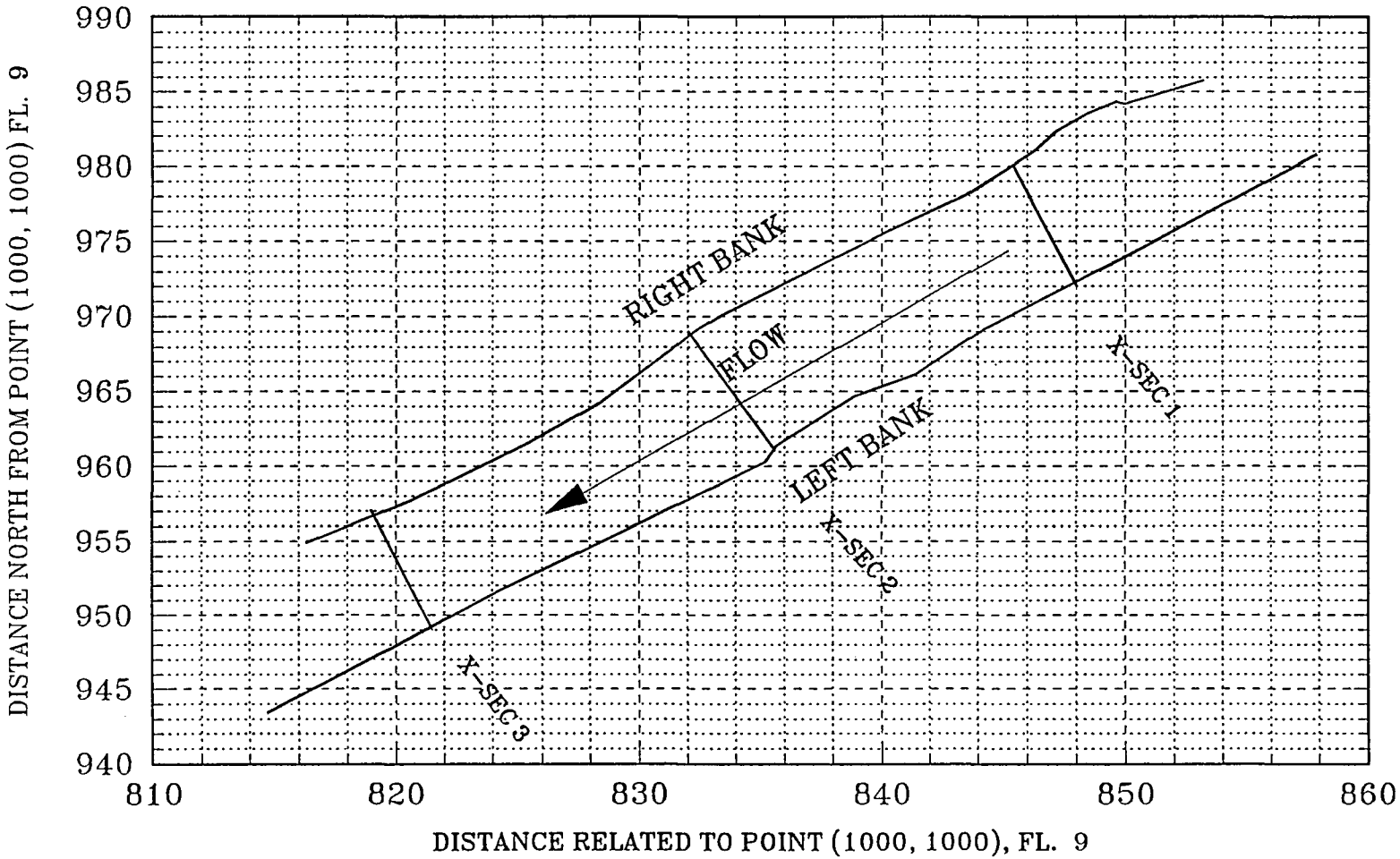

Figure 6

HIGH–WATER MARK SURFACE WATER PROFILE ON BOTH BANKS DOWNSTREAM FL. 9
(FLOOD OF AUGUST 19, 1993)

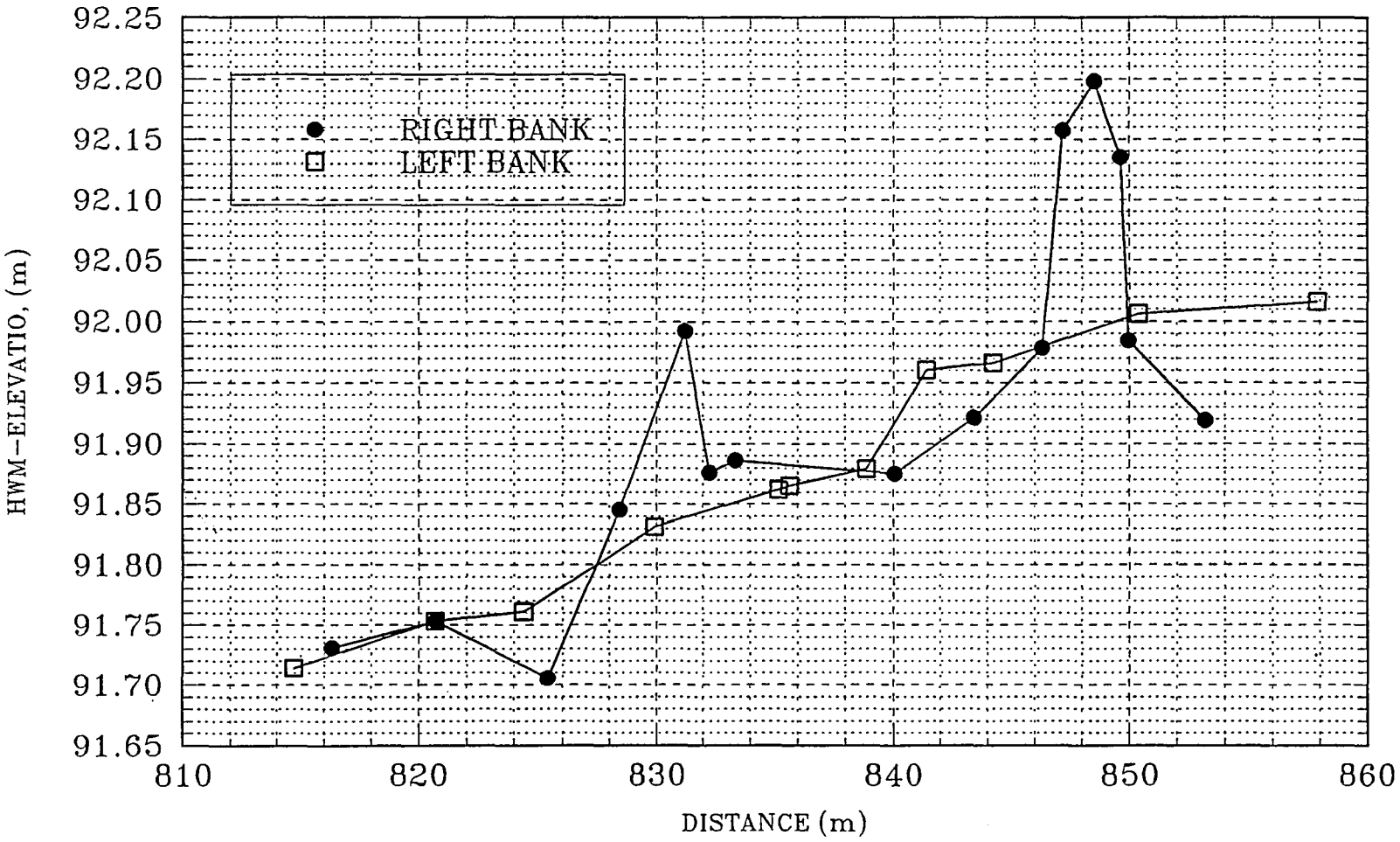

Plate 6a: Photograph looking downstream of the indirect measurement channel reach for the Aug. 19, 1993 event downstream of flume 9.

Plate 6b: Photograph bank collaspe on the right bank of the indirect measurement channel reach for the Aug. 19, 1993 event downstream of flume 9.

Figure 7

HIGH–WATER MARK SURFACE WATER PROFILE ON BOTH BANKS DOWNSTREAM FLUME 6
(FLOOD OF AUGUST 31, 1993)

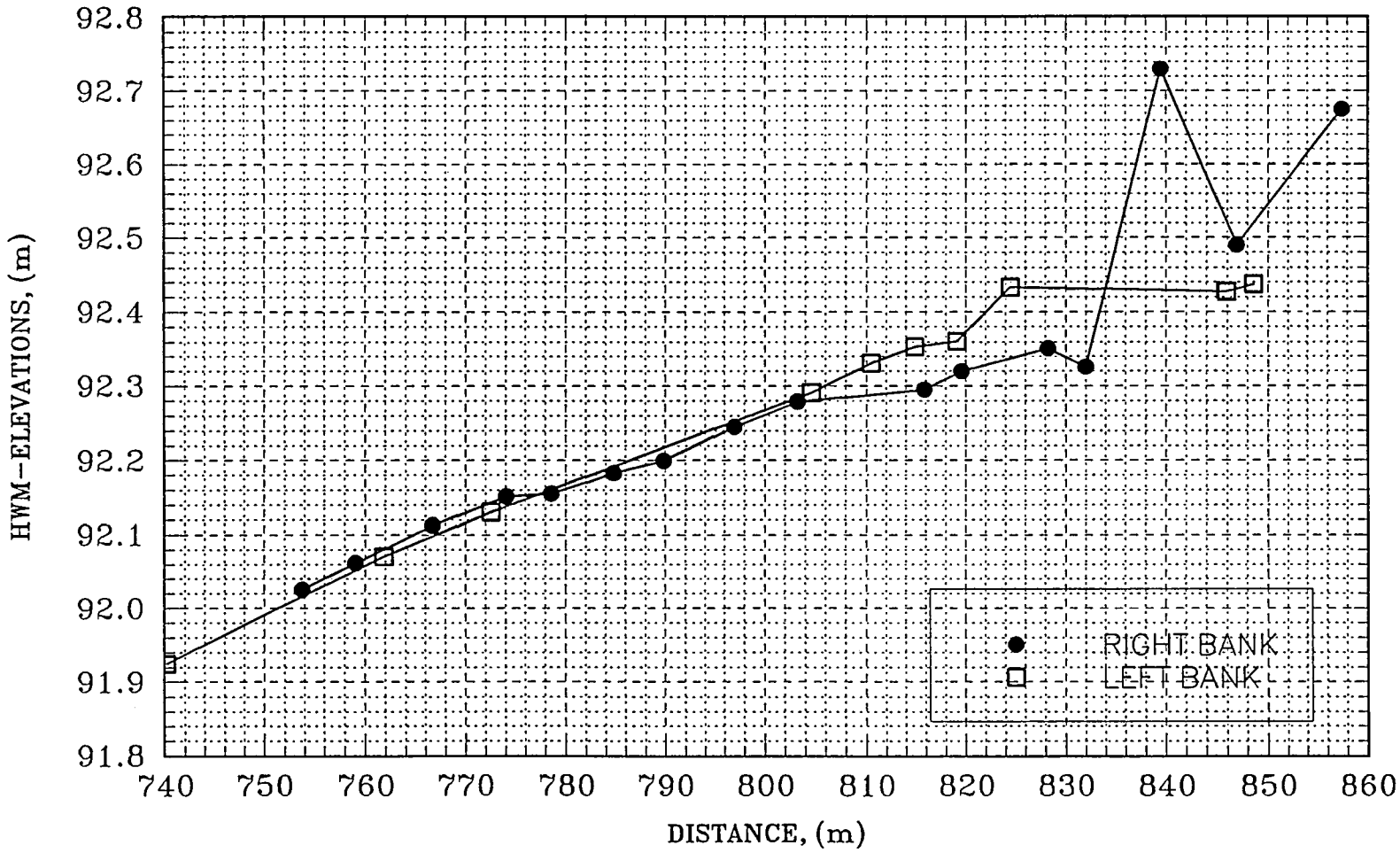

Figure 8a

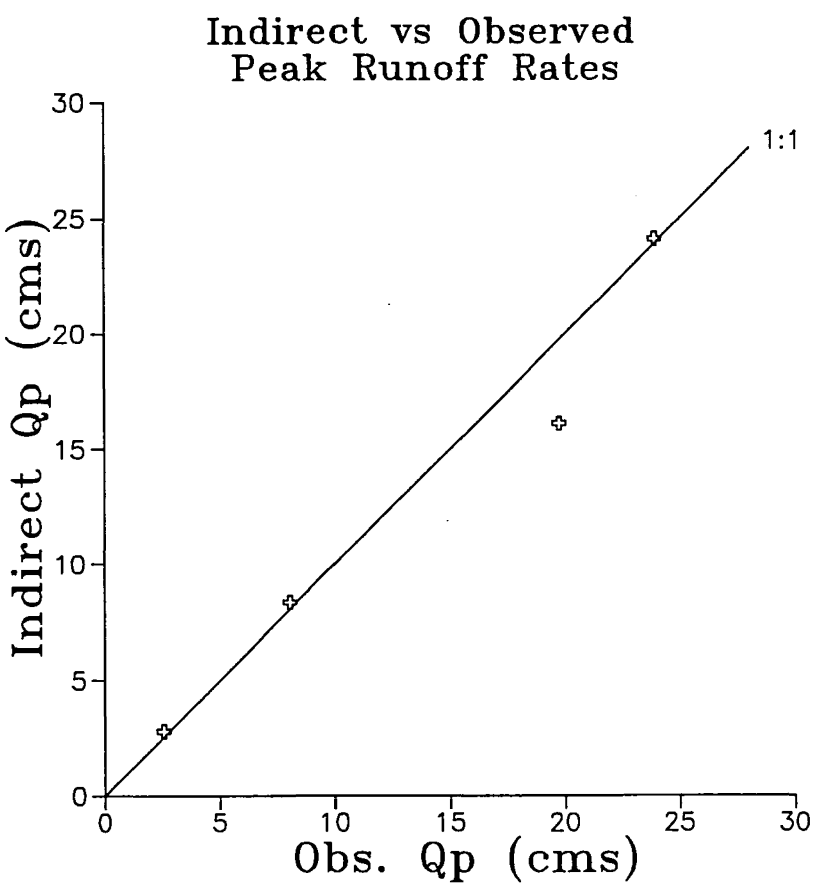

Figure 8b

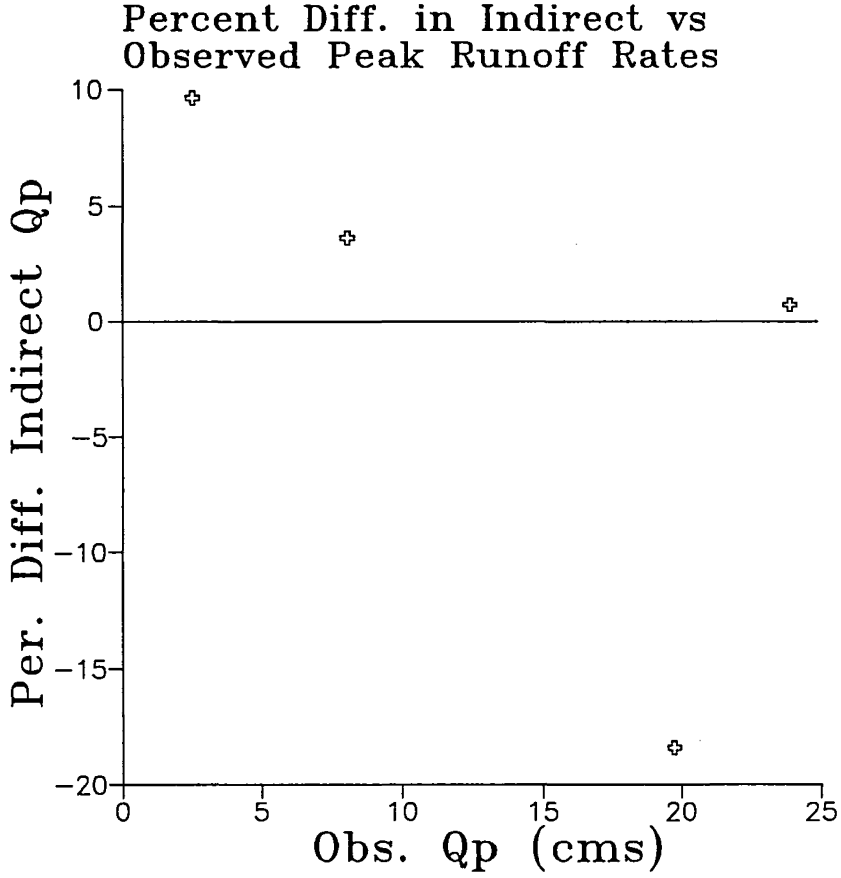

Figure 9

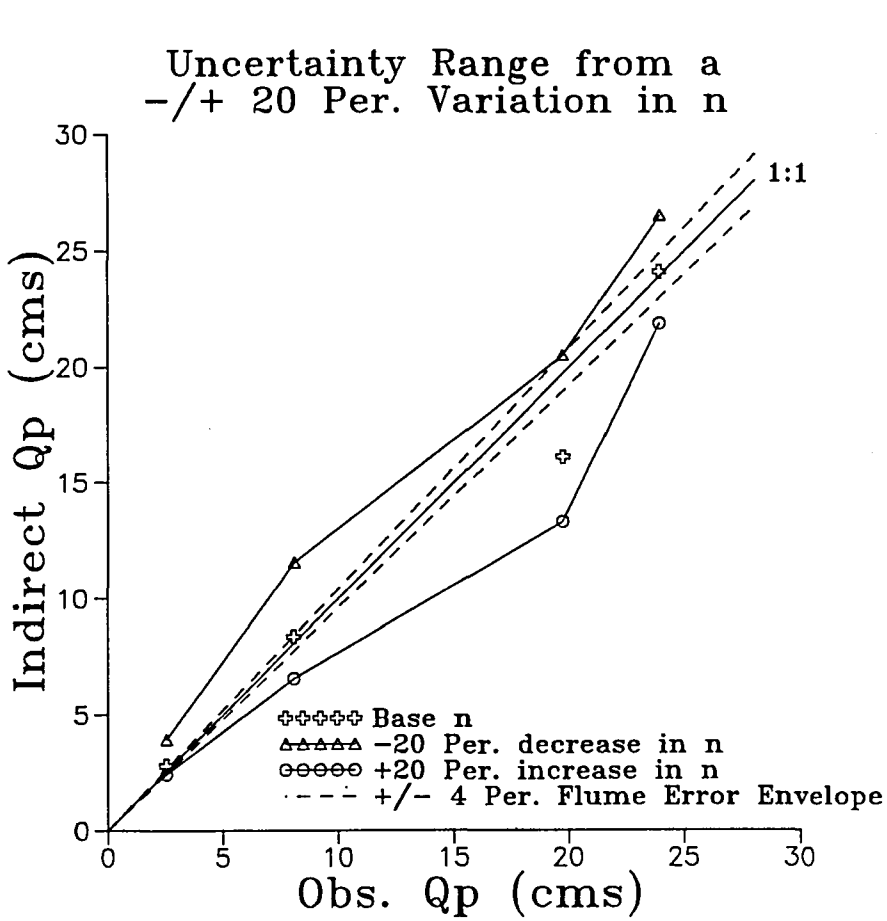

Figure 10

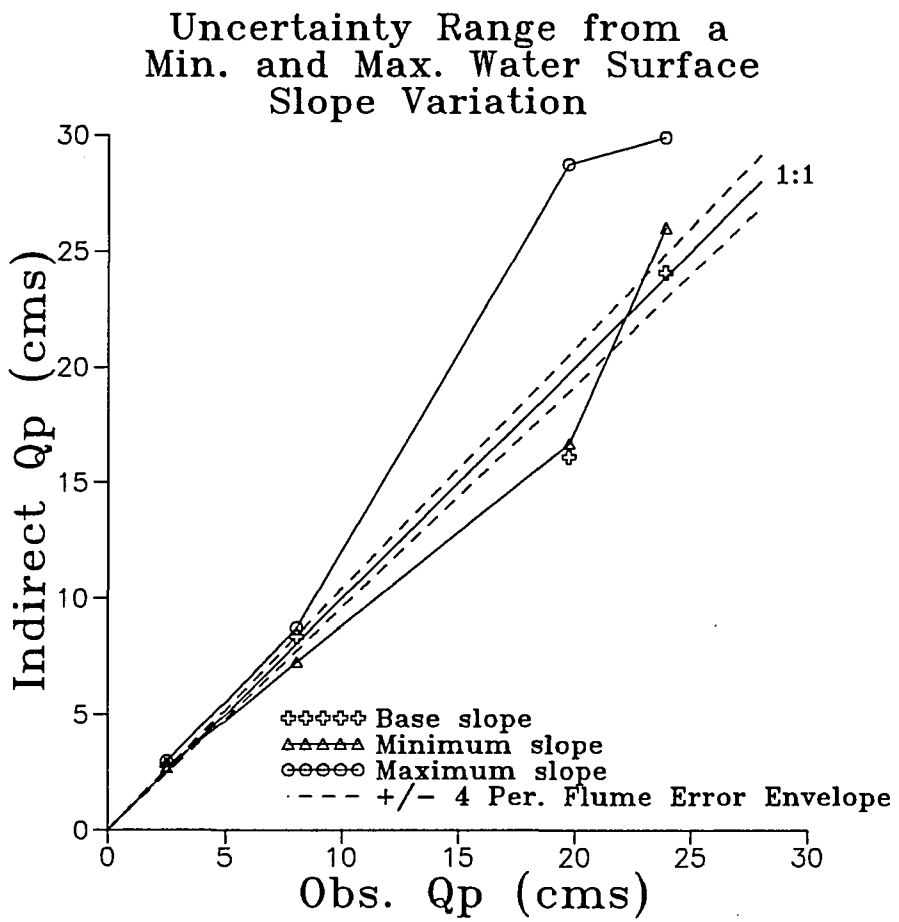

Figure 11

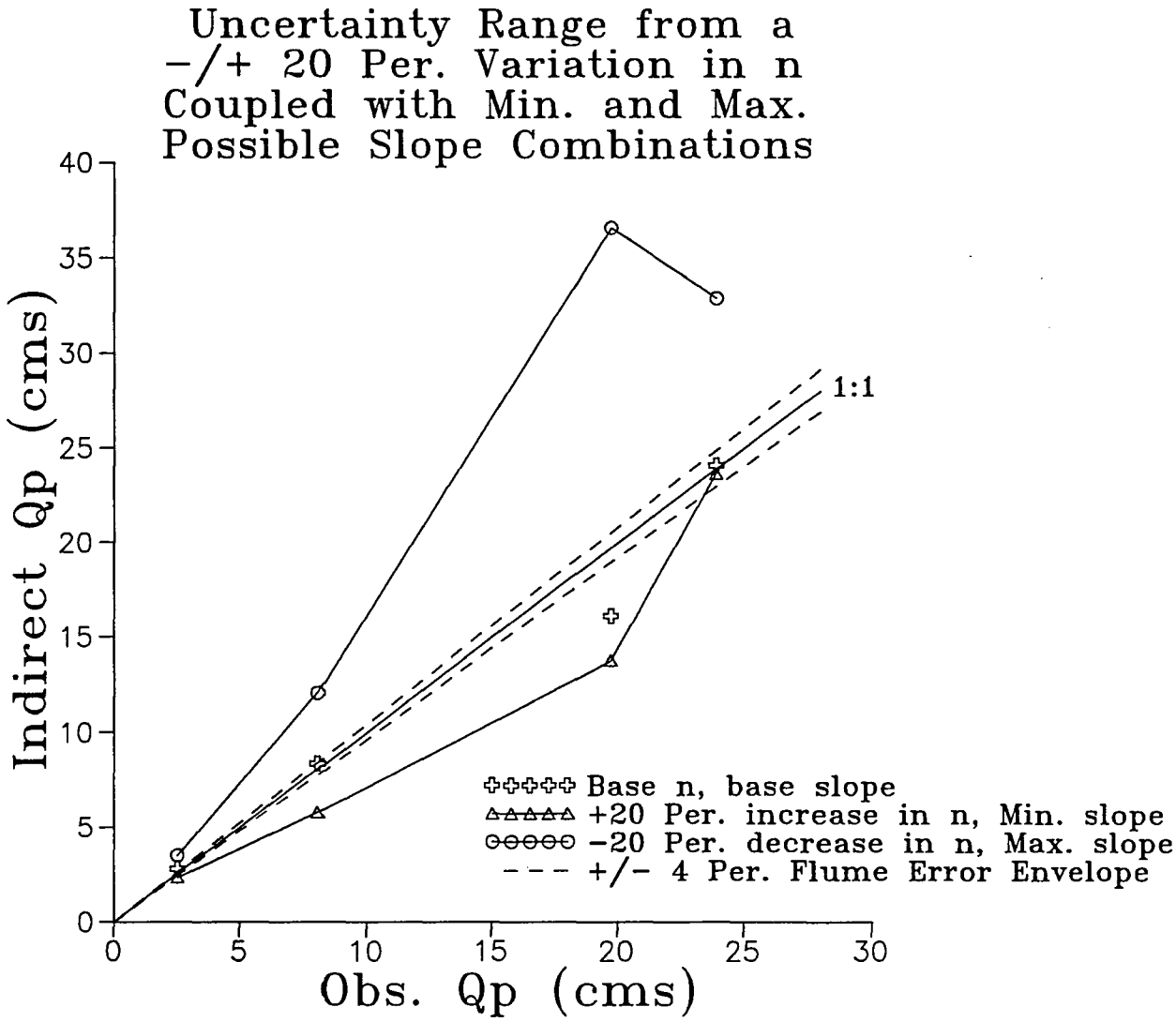
Uncertainty Range from a
−/+ 20 Per. Variation in n
Coupled with Min. and Max.
Possible Slope Combinations
Indirect Qp (cms)
Obs. Qp (cms)
0
5
10
15
20
25
30
35
40
1:1
Base n, base slope
+20 Per. increase in n, Min. slope
−20 Per. decrease in n, Max. slope
+/− 4 Per. Flume Error Envelope

Table 2. Date and Location of Indirect Discharge Measurements

Measurement	Runoff Event Date	Meas. Date	Location
1	Aug. 19, 1993	Aug. 23, 1993	Downstream of Flume 9
2	Aug. 19, 1993	Aug. 23, 1993	Upstream of Flume 10
3	Aug. 31, 1993	Sept. 1, 1993	Downstream of Flume 9
4	Aug. 31, 1993	Sept. 1, 1993	Downstream of Flume 6

Table 3: Manning's hydraulic roughness estimate for each cross section of each indirect measurement and typical published ranges of hydraulic roughness for the material typical of the cross sections.

Meas./Date/Fl. #	Cross Section (1-Upstream)	Hydraulic Roughness (n)[1] (channel/overbank)	Published Range of (n)[1] (channel/overbank)
1 / 8-19-93 / 9	1	0.025/0.04	0.012-0.03/0.035-0.06
	2	0.025/0.04	0.012-0.03/0.035-0.06
	3	0.025/0.04	0.012-0.03/0.035-0.06
2 / 8-19-93 / 10	1	0.025	0.012-0.03
	2	0.025	0.012-0.03
	3	0.025	0.012-0.03
3 / 8-31-93 / 9	1	0.025/0.04	0.012-0.03/0.035-0.06
	2	0.025/0.04	0.012-0.03/0.035-0.06
	3	0.025/0.04	0.012-0.03/0.035-0.06
4 / 8-31-93 / 6	1	0.03	0.03-0.04
	2	0.03	0.03-0.04
	3	0.03	0.03-0.04

[1] Manning's Roughness Value (Chow, 1959; Woolhiser et al., 1990)

Table 4. Summary of Observed and Indirect Peak Discharge Measurements (Qp)

Meas./Date/Fl. #	Obs. Stage (m)	Obs. Qp (m^3/s)	Indirect (Qp) (m^3/s)	Percent Diff.[1]
1 / 8-19-93 / 9	0.524	8.08	8.37	3.62
2 / 8-19-93 / 10	0.304	2.55	2.80	9.64
3 / 8-31-93 / 9	0.881	23.92	24.09	0.71
4 / 8-31-93 / 6	0.777	19.73	16.10	-18.39

[1] (Indirect Qp - Obs. Qp) / (Obs. Qp) X 100

Table 5. Summary Statistics of Variation in Indirect Peak Discharge Due to Variation in Hydraulic Roughness, Slope, and Combinations of Roughness and Slope

Parameter Deviation	Mean of Abs. Diff. from Observed Qp (m^3/s)[1]	Mean of Abs. Percentage Diff. from Obs. Qp[2]
Base roughness and slope	1.09	8.09
20% increase in roughness	2.53	16.02
20% decrease in roughness	2.04	21.60
Maximum slope	4.02	23.92
Minimun slope	1.53	10.00
20% increase in roughness and minimum slope	2.19	17.07
20% decrease in roughness and maximum slope	7.70	52.15

[1] Sum (abs(Indirect Qp - Obs. Qp)) / 4
[2] Sum (abs(Indirect Qp - Obs. Qp)) / (Obs. Qp X 100) / 4

Appendix A:

Figures of the:

1) Plan view of high-water marks;

2) High-water mark surface water profiles on both banks

3) Channel cross-sections,

for each for the four indirect measurements.

LAYOUT FOR HIGH–WATER MARKS DOWNSTREAM FLUME 9
(FLOOD OF 19 AUGUST 1993)

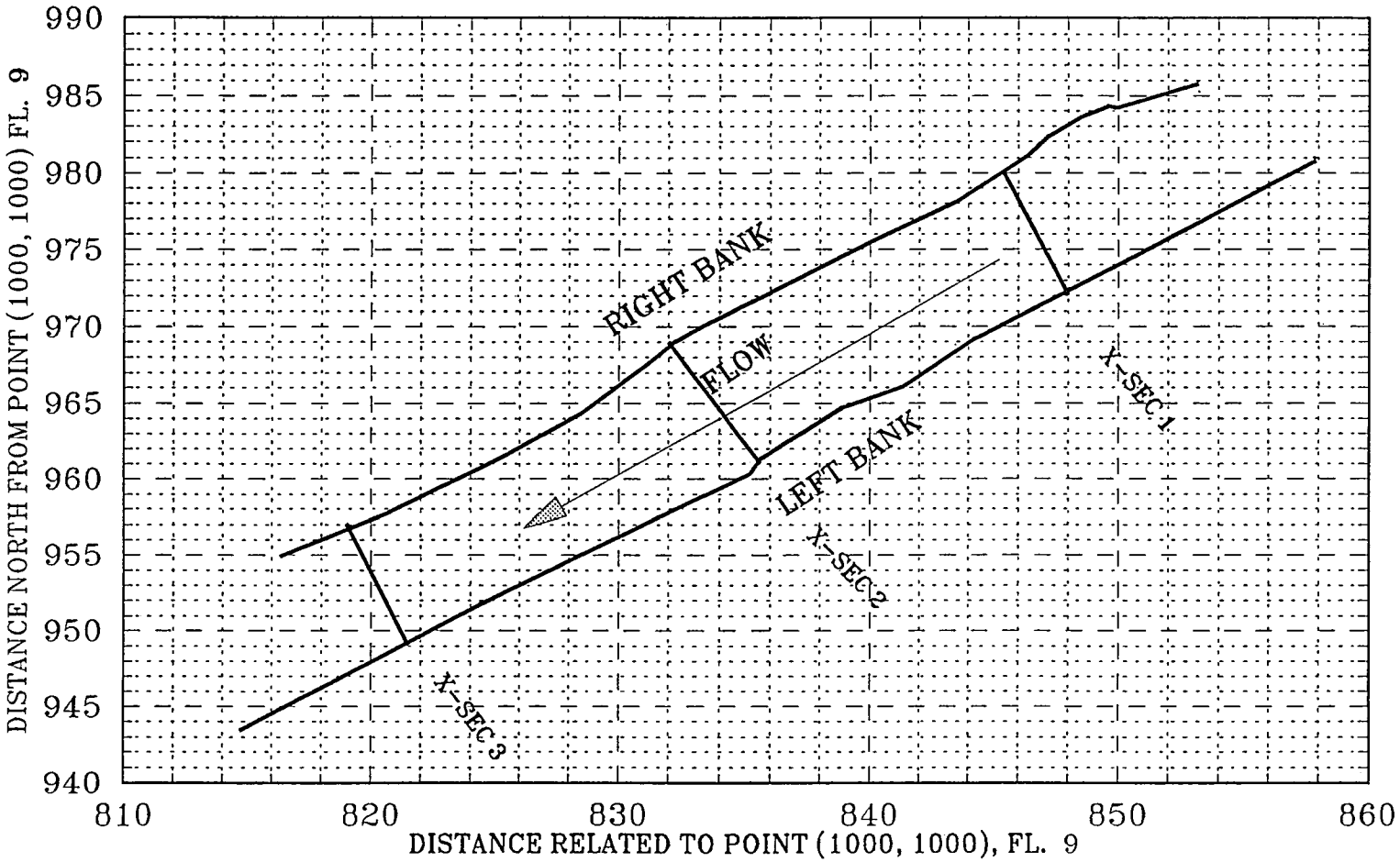

HIGH–WATER MARKS ELEVATION ON BOTH BANKS DOWNSTREAM FL. 9
(FLOOD OF AUGUST 19, 1993)

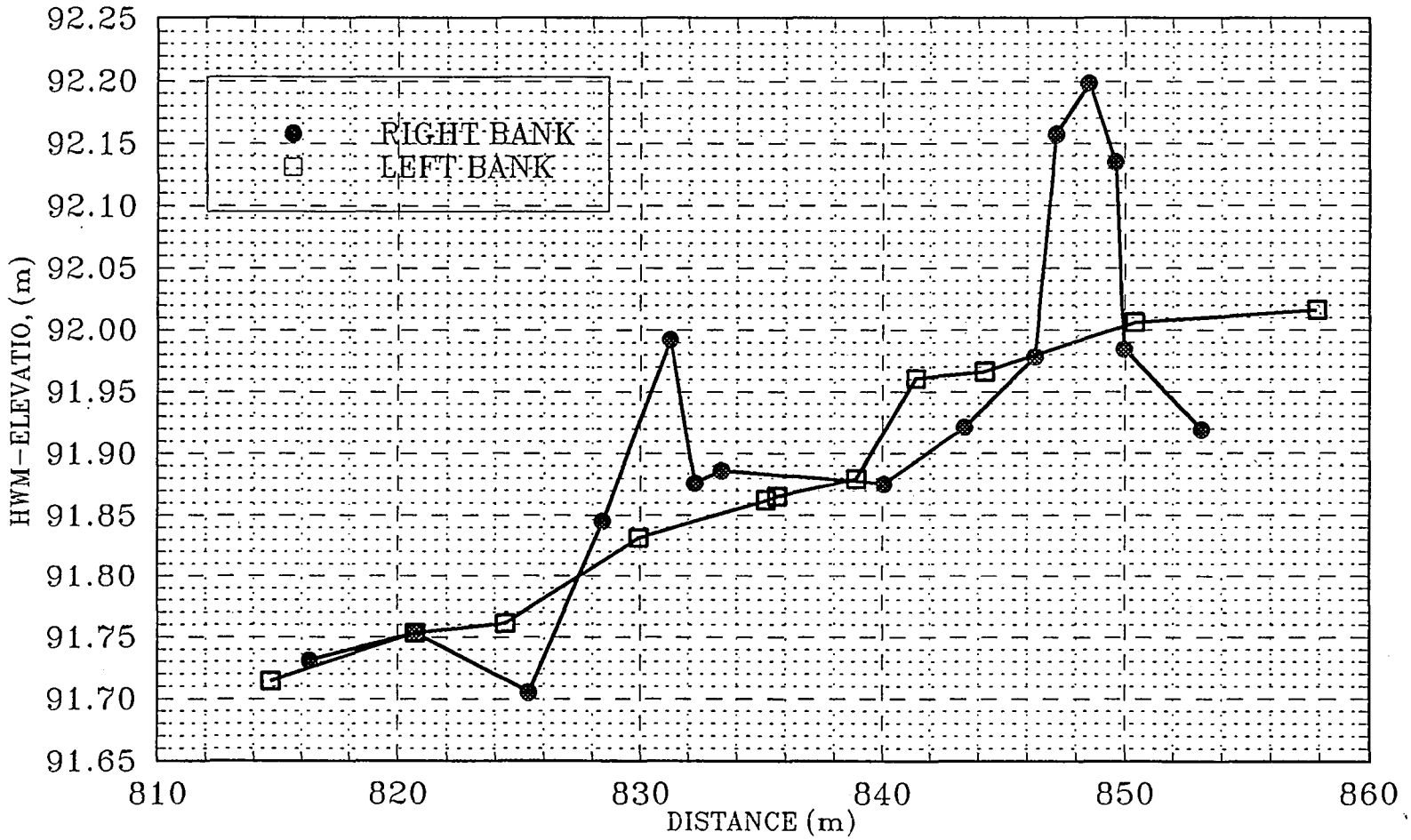

X-SEC. 1 DOWNSTREAM FLUME 9
(FLOOD OF AUGUST 19, 1993)

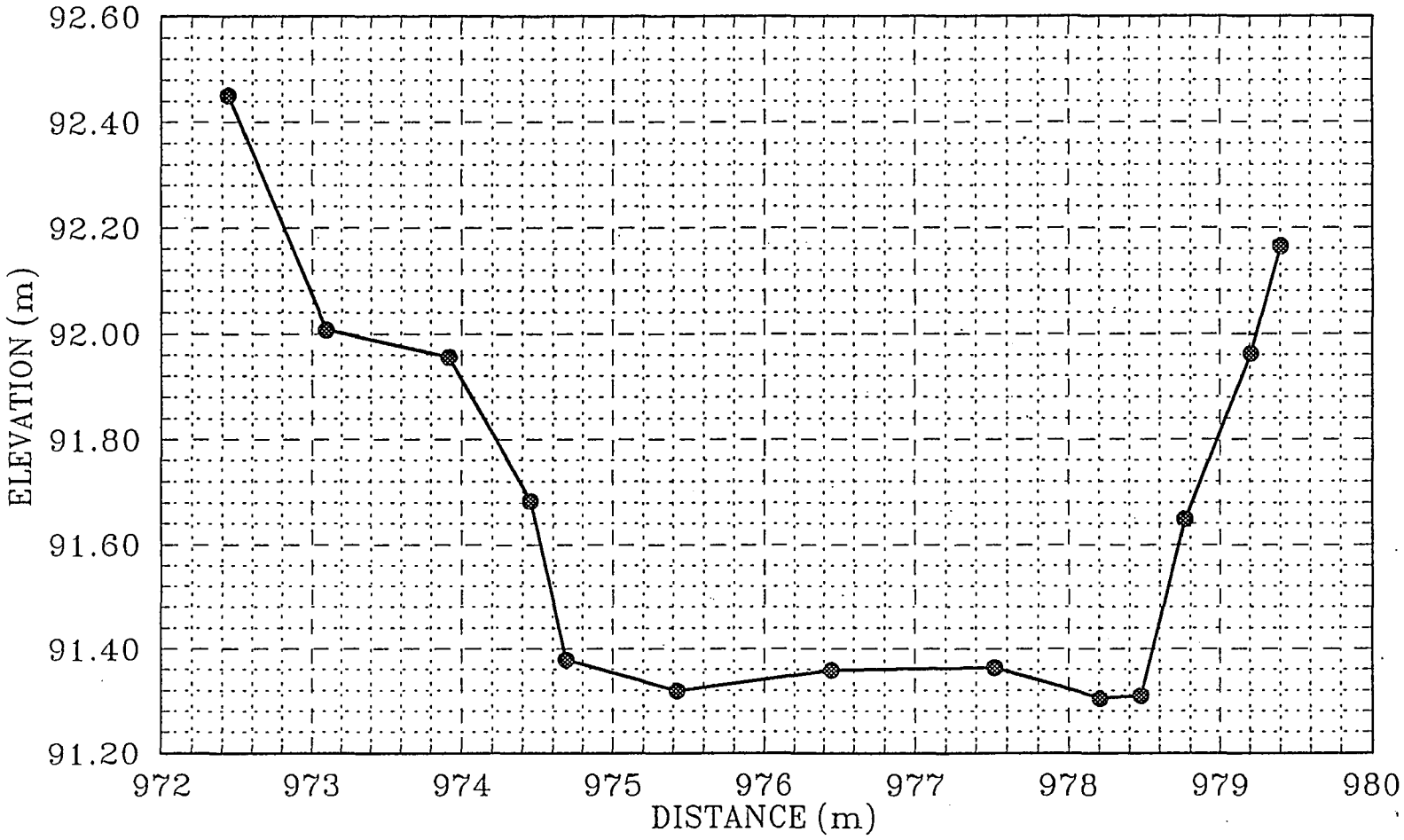

X-SEC. 2 DOWNSTREAM FLUME 9
(FLOOD OF AUGUST 19, 1993)

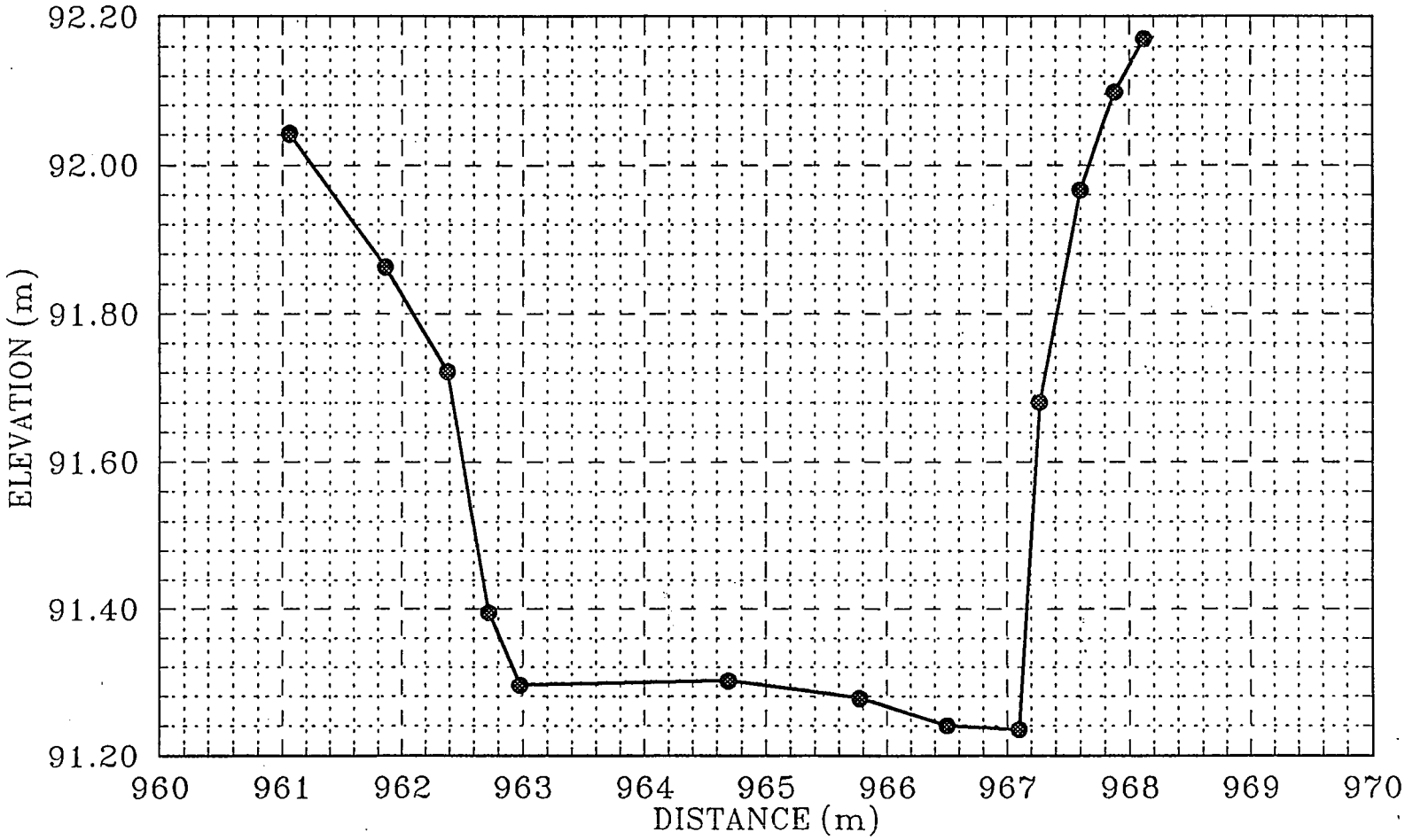

X-SEC. 3 DOWNSTREAM FLUME 9
(FLOOD OF AUGUST 19, 1993)

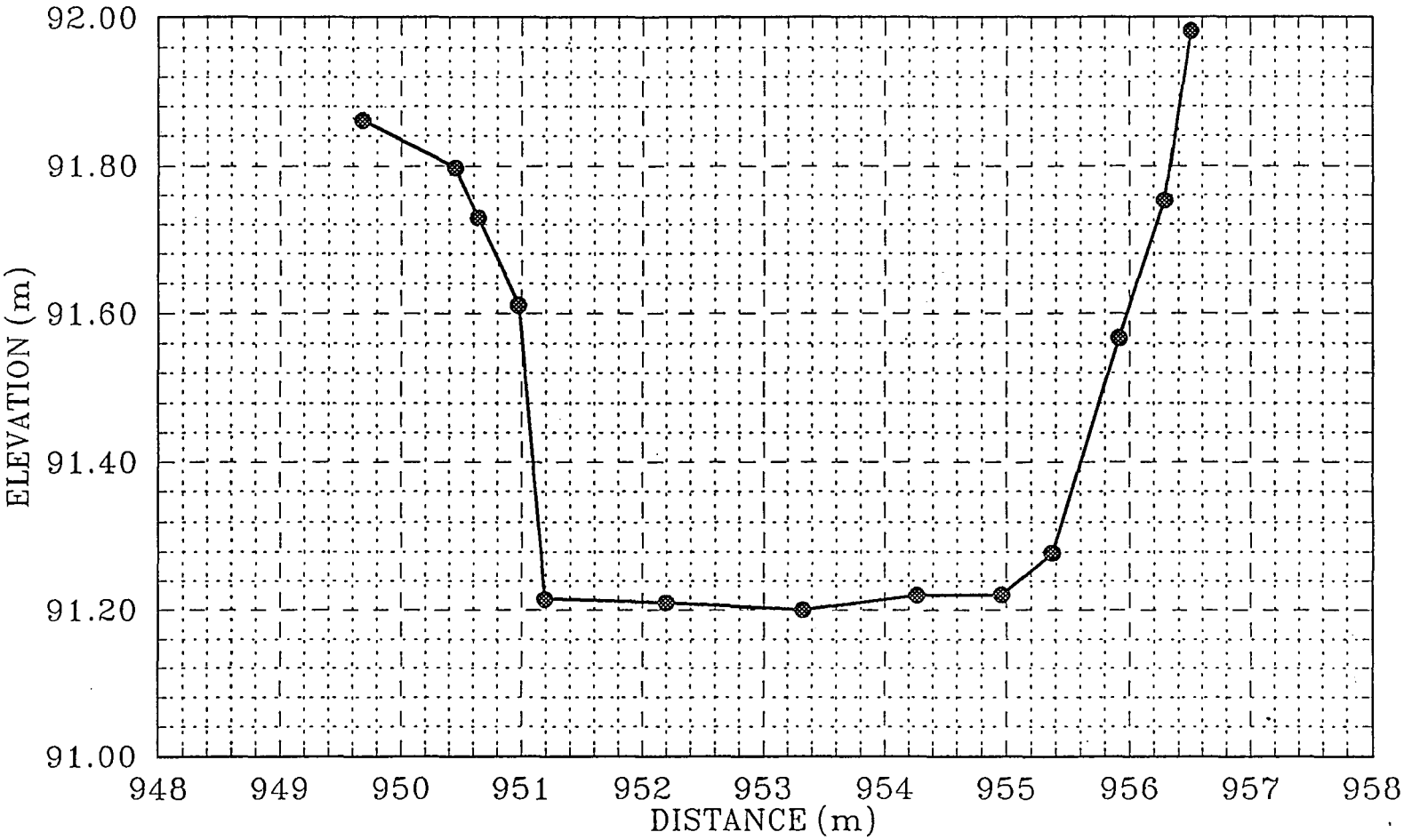

LAYOUT FOR HIGH–WATER MARKS UPSTREAM FLUME 10
(FLOOD OF 19 AUGUST 1993)

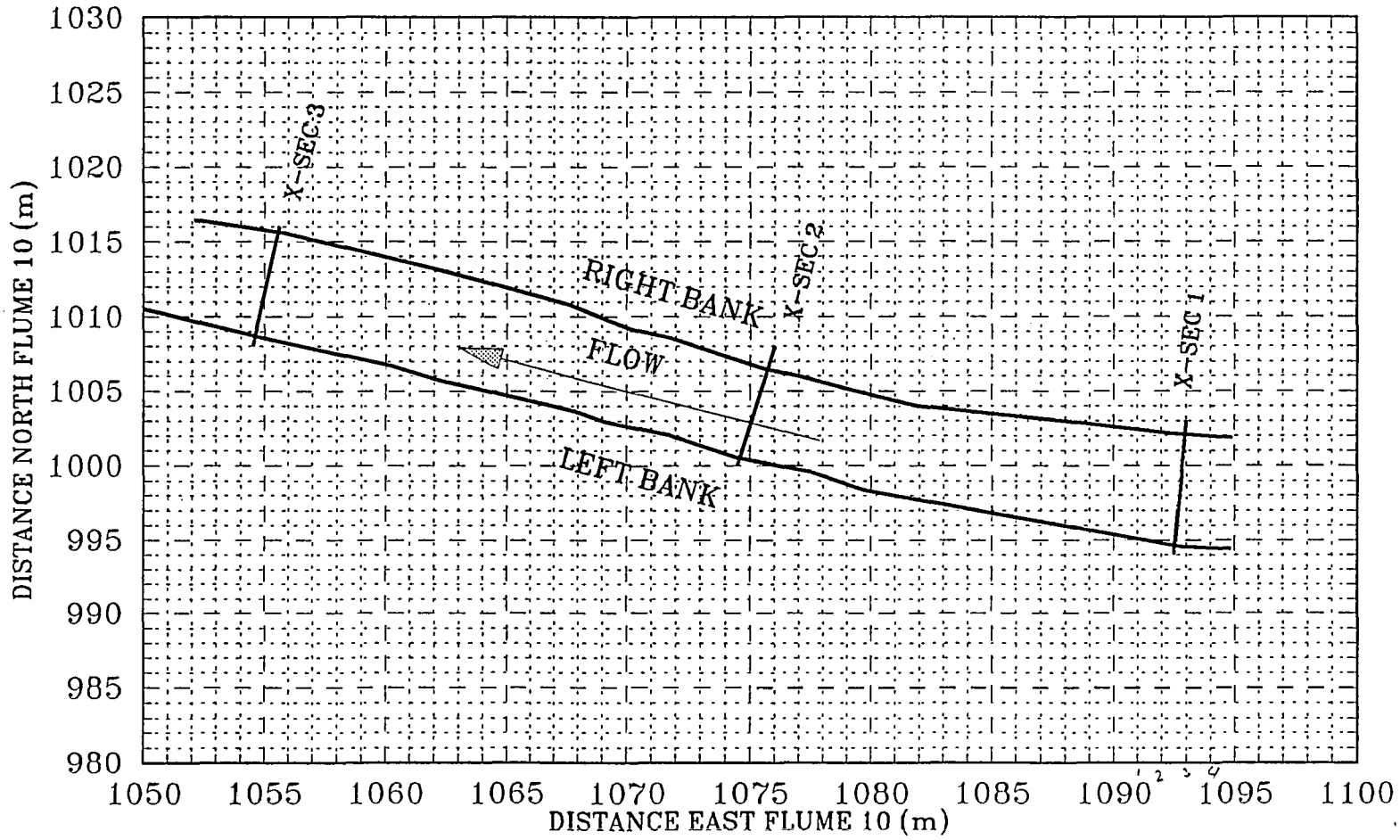

HIGH–WATER MARKS ELEVATION ON BOTH BANKS UPSTREAM FLUME 10
(FLOOD OF 19 AUGUST 1993)

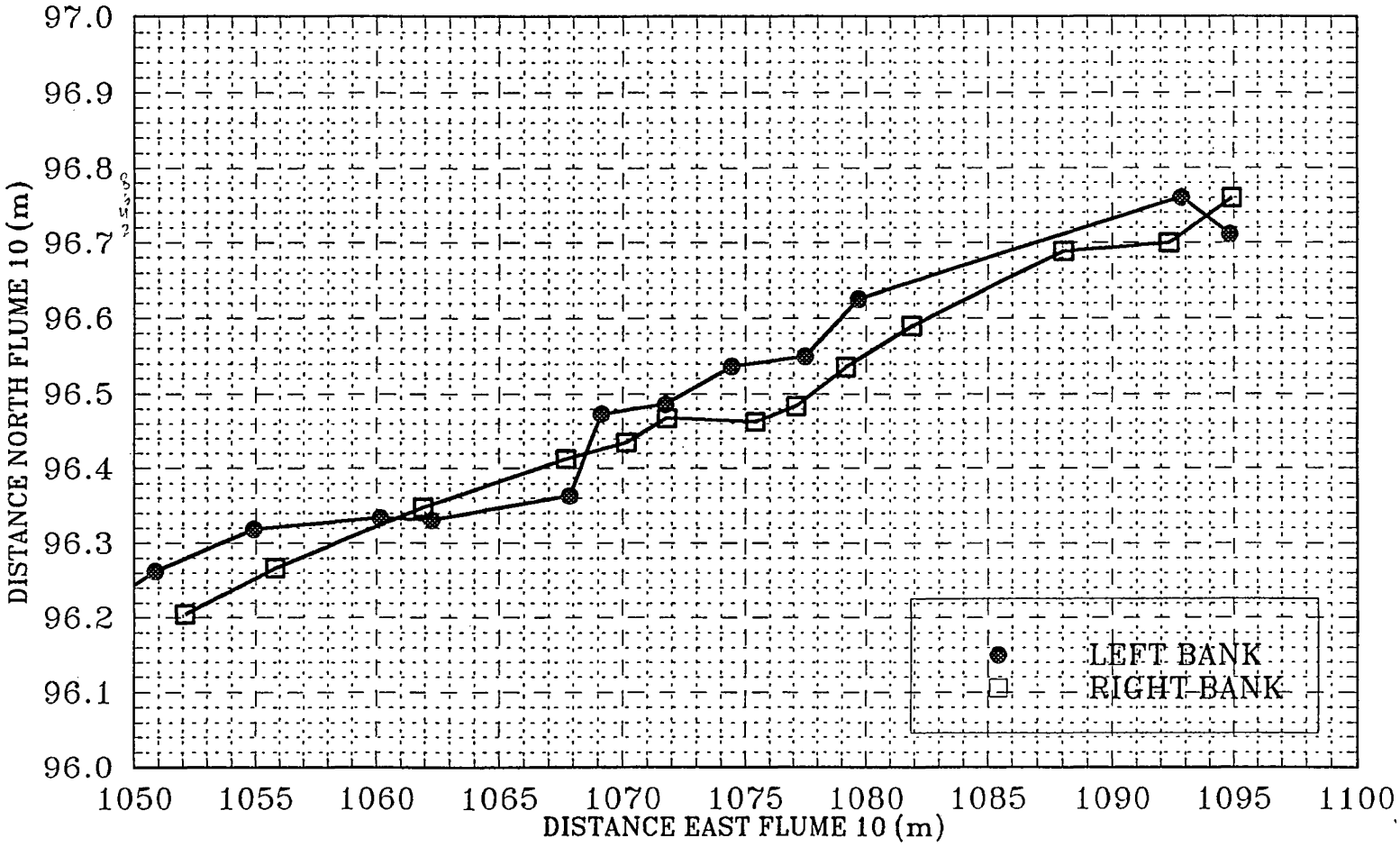

X-SEC. 1 UPSTREAM FLUME 10
(FLOOD OF AUGUST 19, 1993)

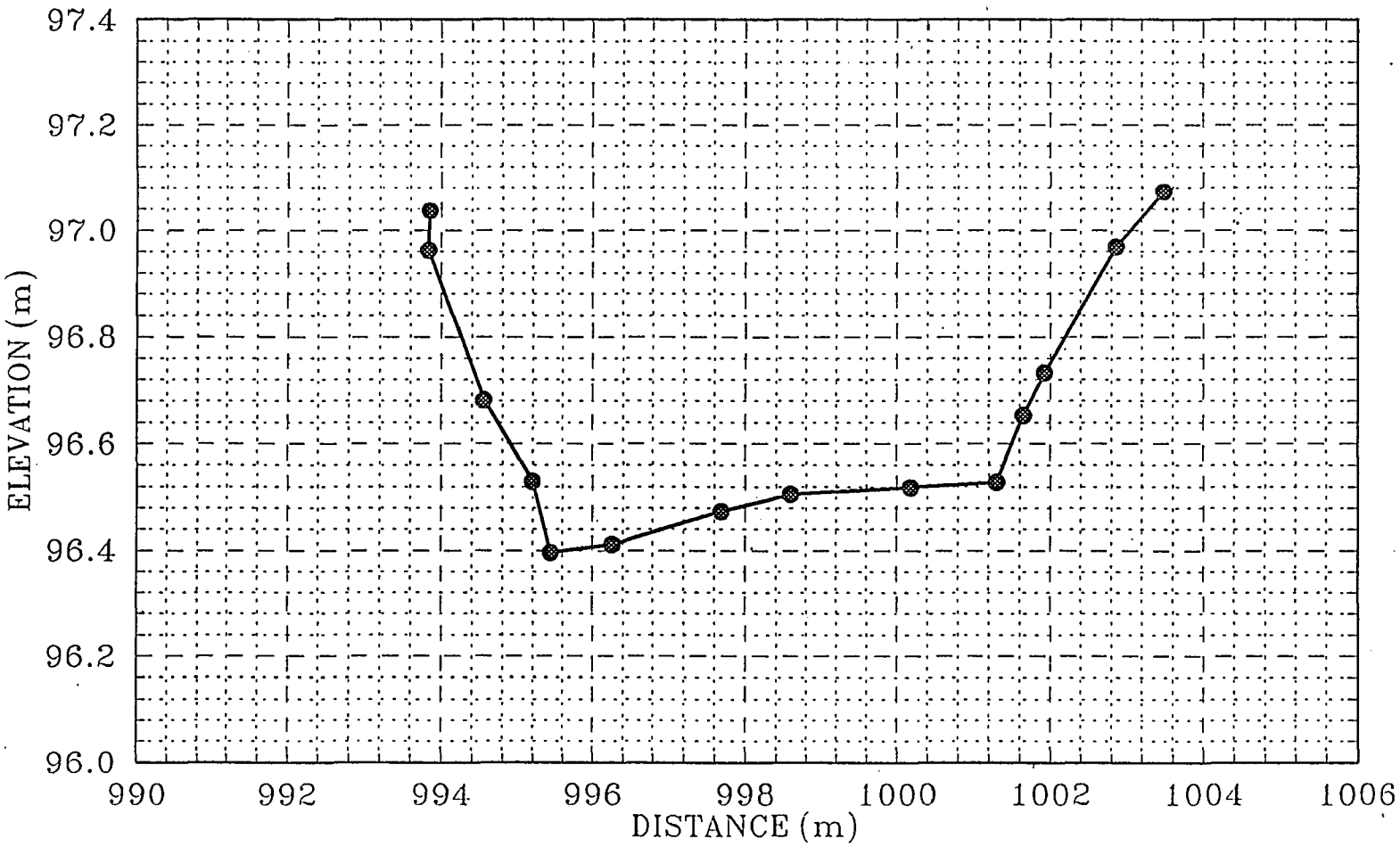

X-SEC. 2 UPSTREAM FLUME 10
(FLOOD OF AUGUST 19, 1993)

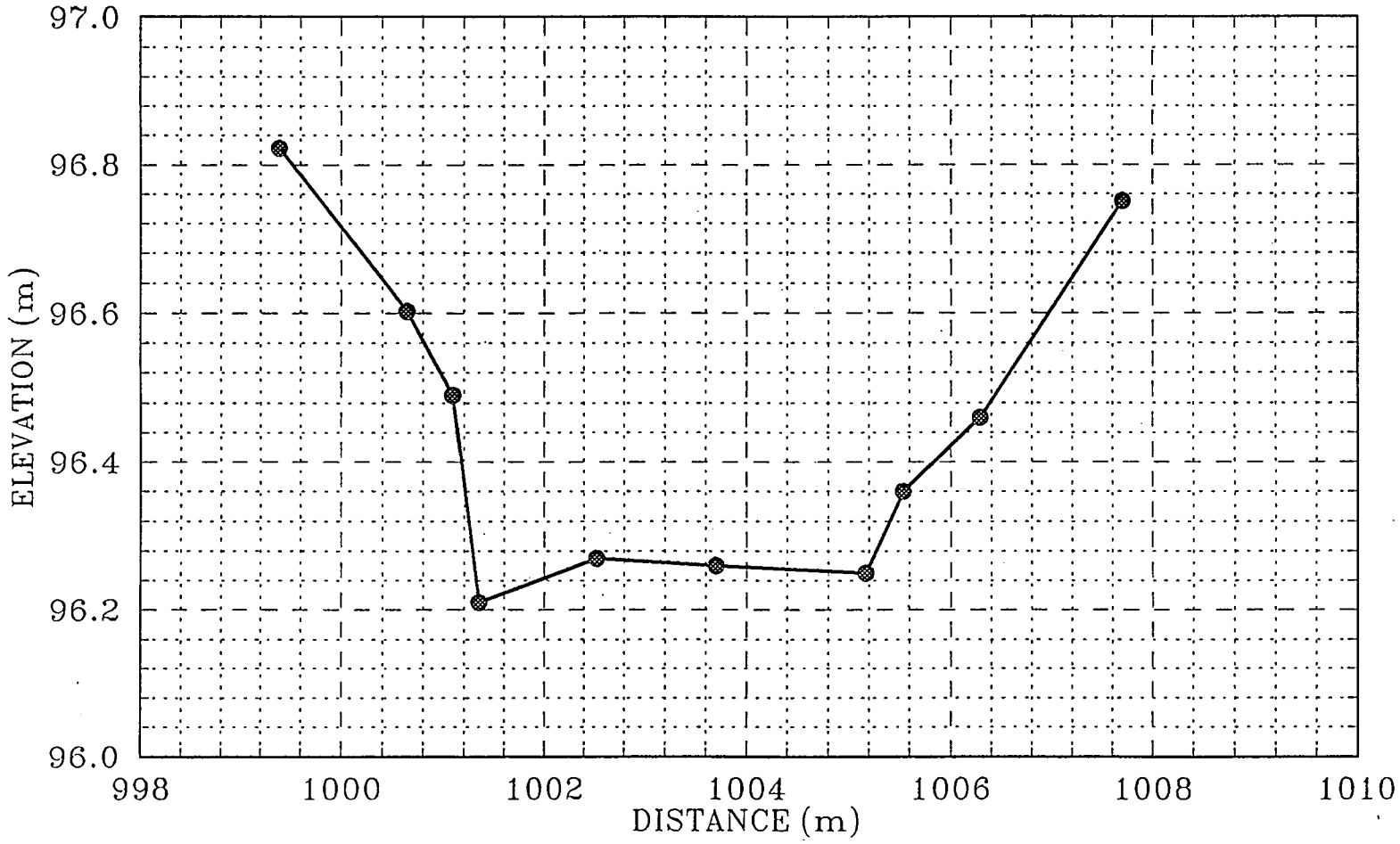

X-SEC. 3 UPSTREAM FLUME 10
(FLOOD OF AUGUST 19, 1993)

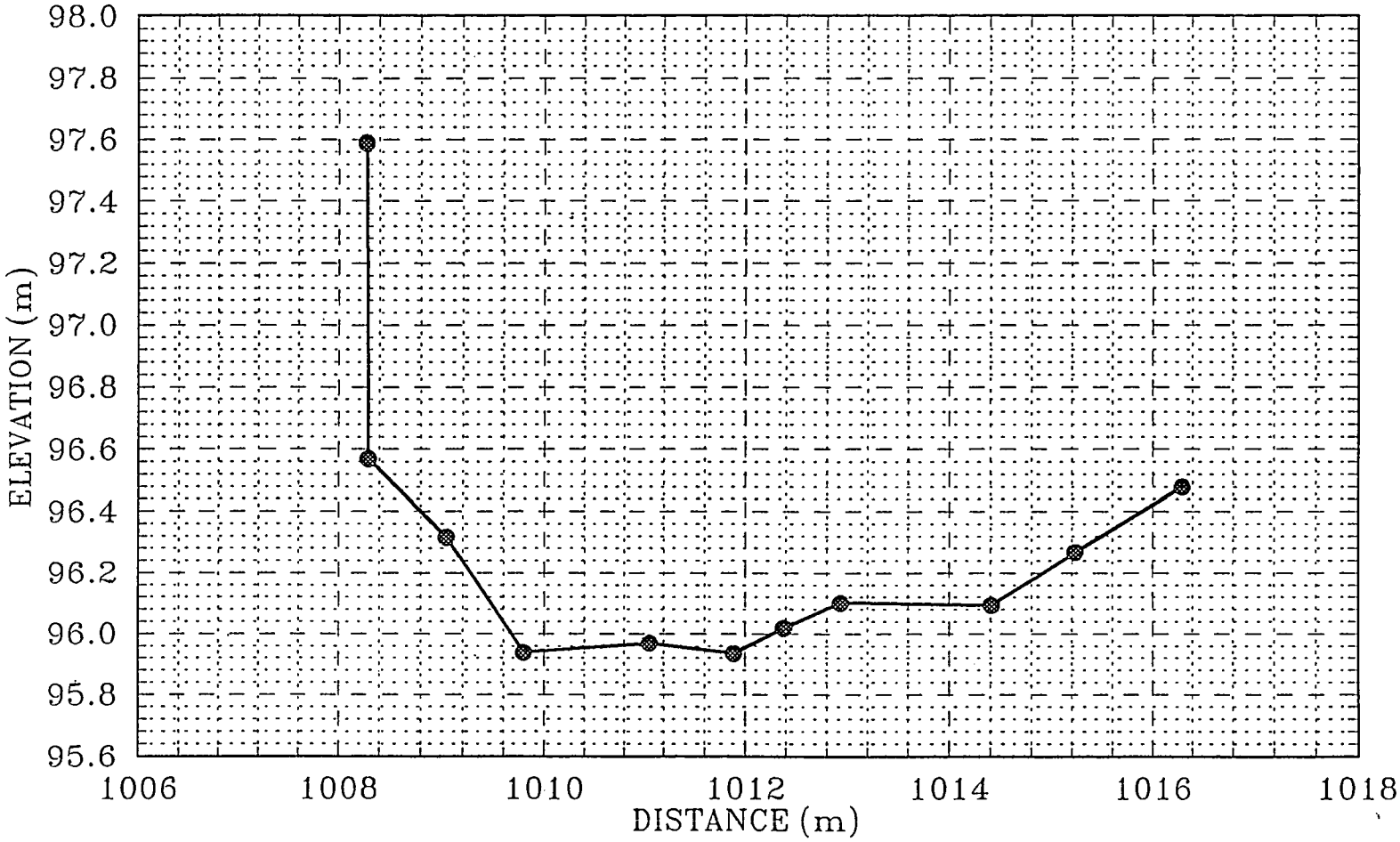

LAYOUT FOR HIGH–WATER MARKS DOWNSTREAM FLUME 6
(FLOOD OF AUGUST 31, 1993)

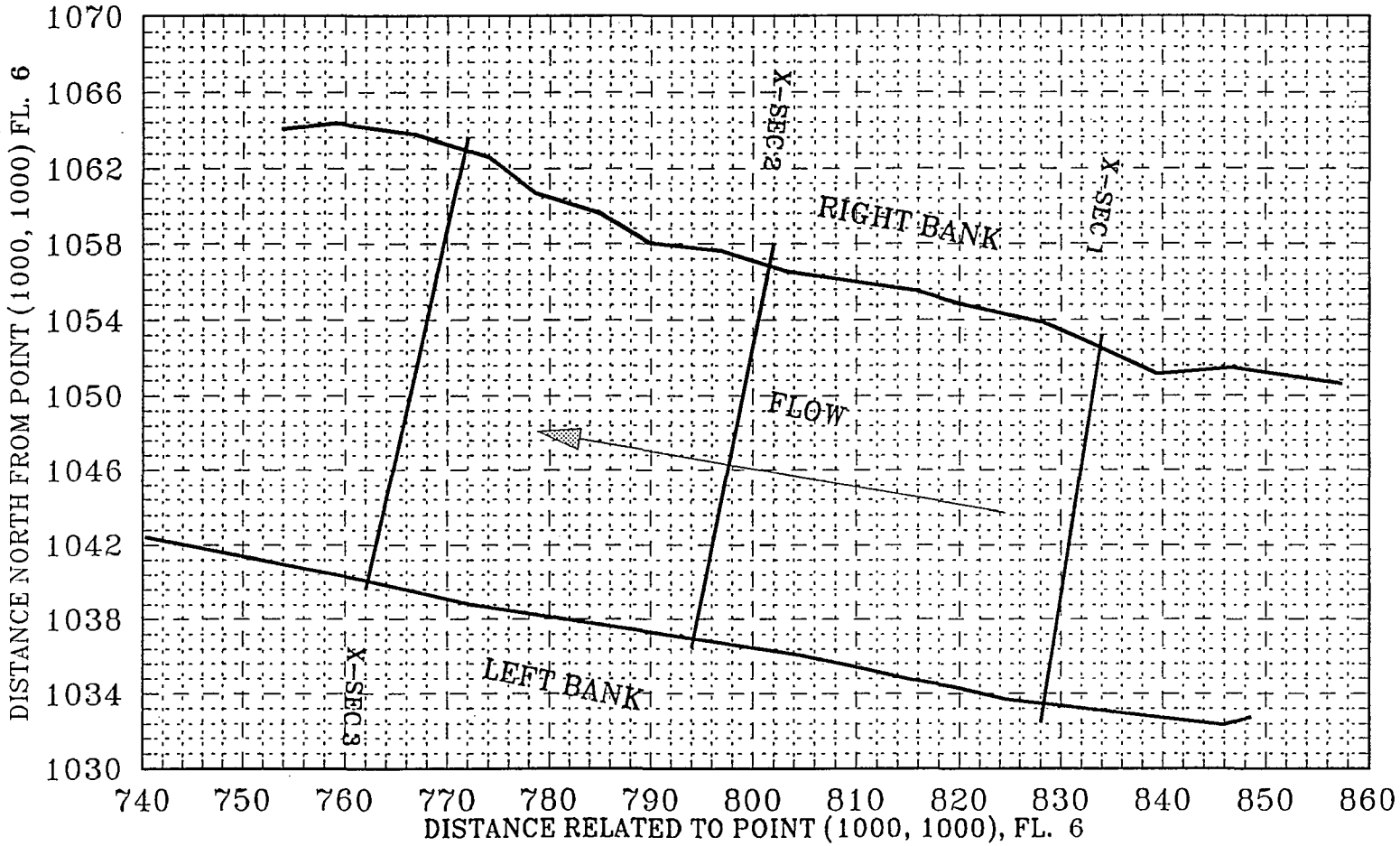

HIGH–WATER MARKS ELEVATIONS ON BOTH BANKS DOWNSTREAM FLUME 6
(FLOOD OF AUGUST 31, 1993)

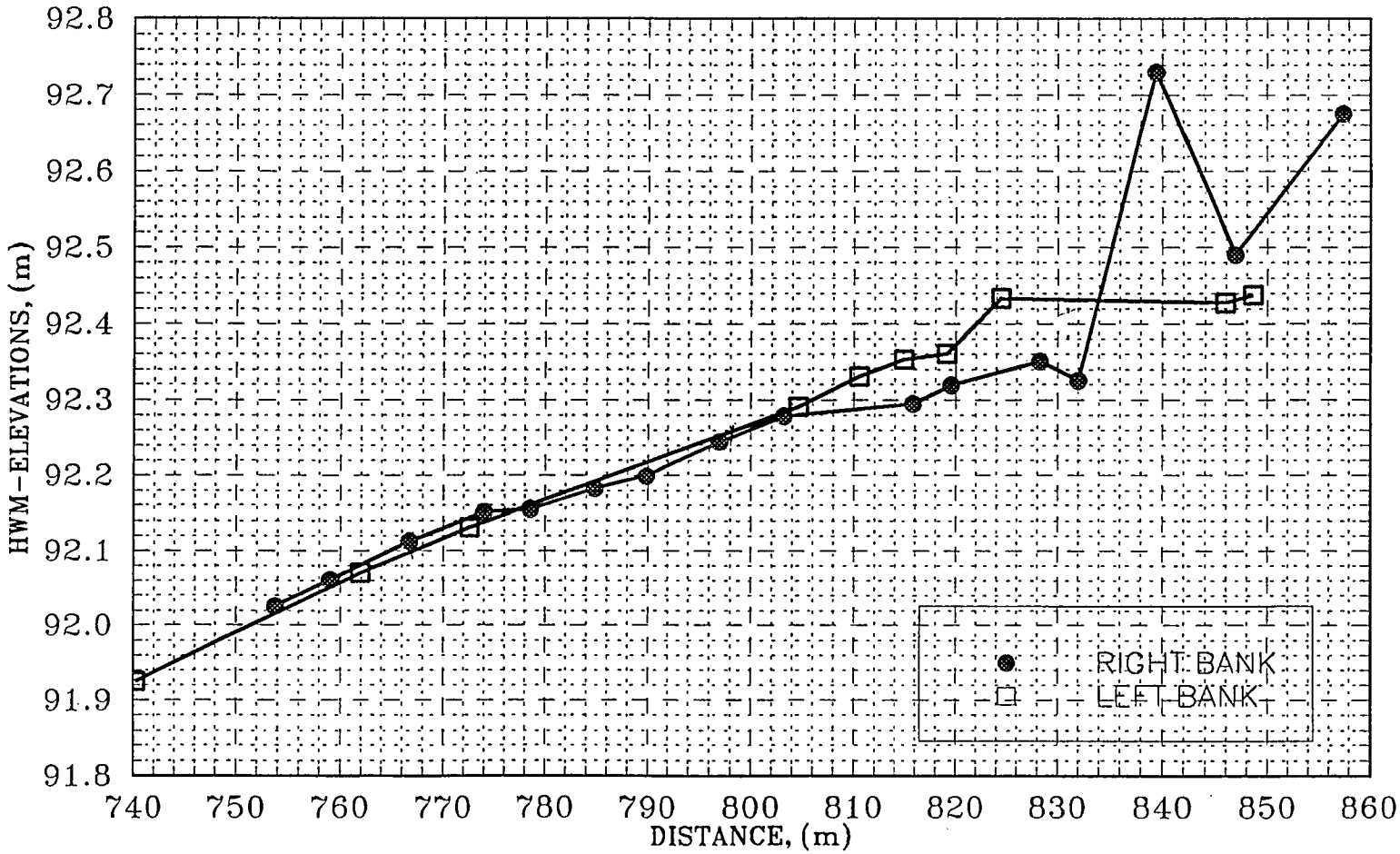

X–SEC. 1 DOWN–STREAM FLUME 6
(FLOOD OF AUGUST 31, 1993)

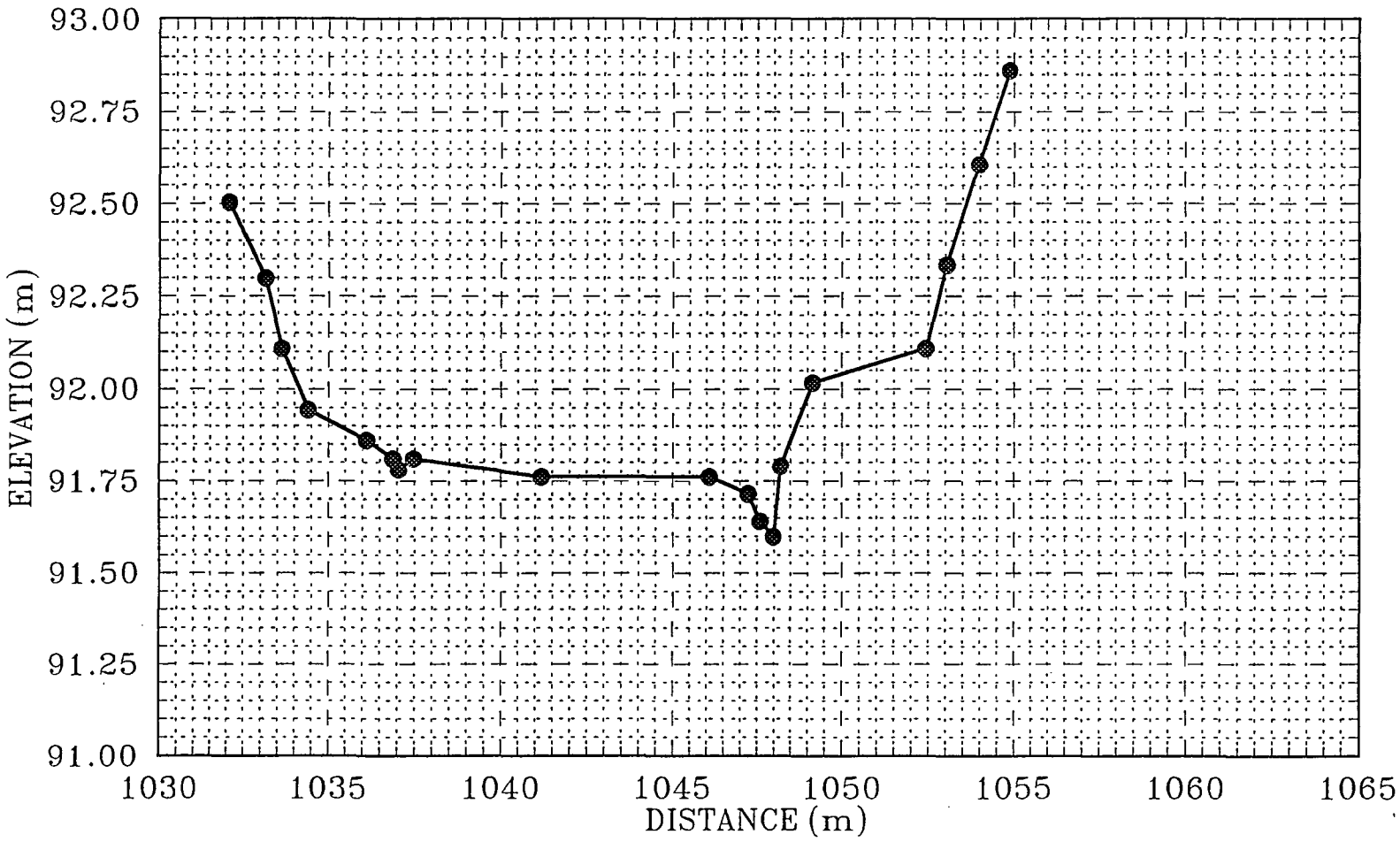

X-SEC. 2 DOWN-STREAM FLUME 6
(FLOOD OF AUGUST 31, 1993)

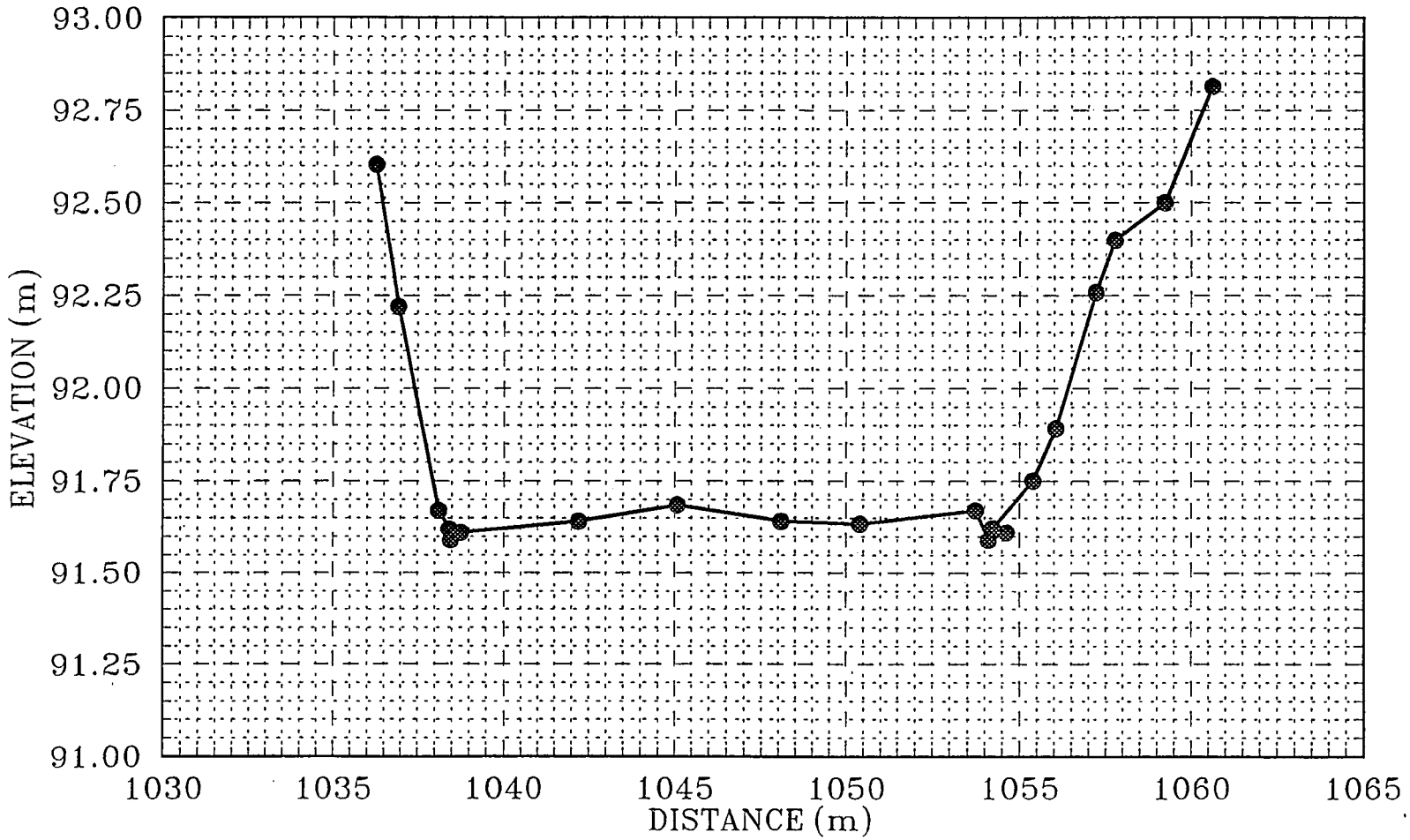

X-SEC. 3 DOWN-STREAM FLUME 6
(FLOOD OF AUGUST 31, 1993)

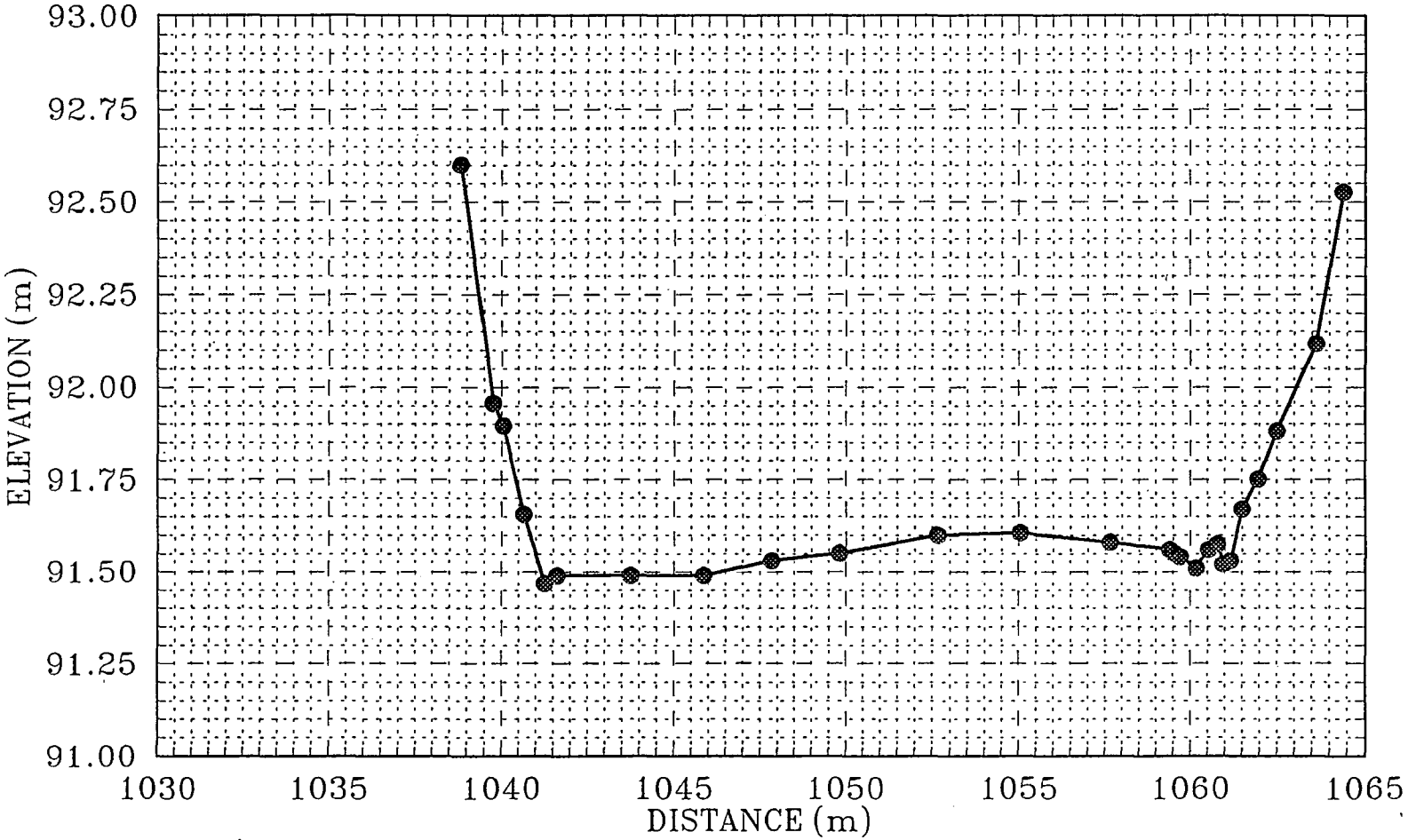

LAYOUT FOR HIGH–WATER MARKS DOWNSTREAM FLUME 9
(FLOOD OF AUGUST 31, 1993)

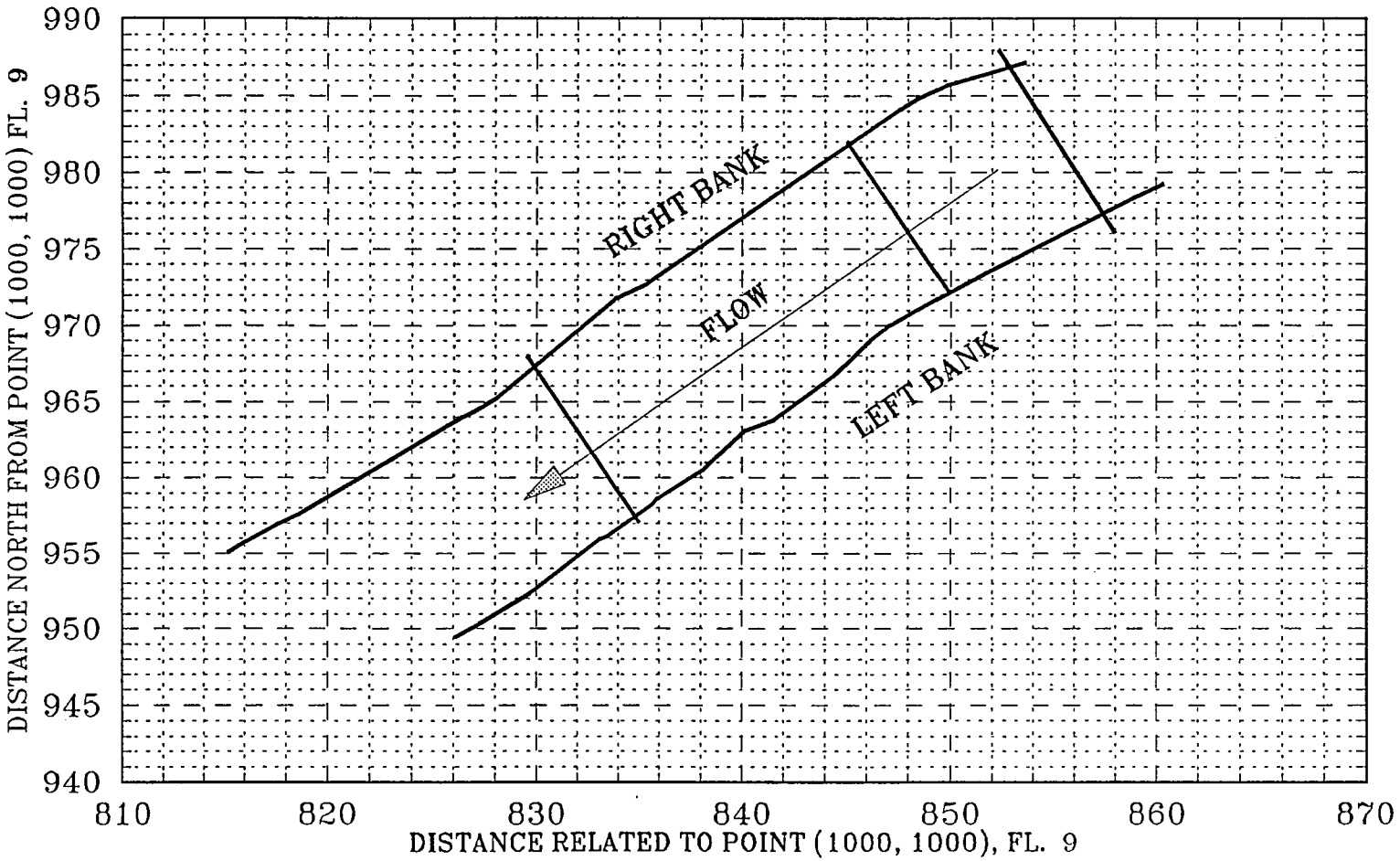

HIGH–WATER MARKS ELEVATION ON BOTH BANKS DOWNSTREAM FL. 9
(FLOOD OF AUGUST 31, 1993)

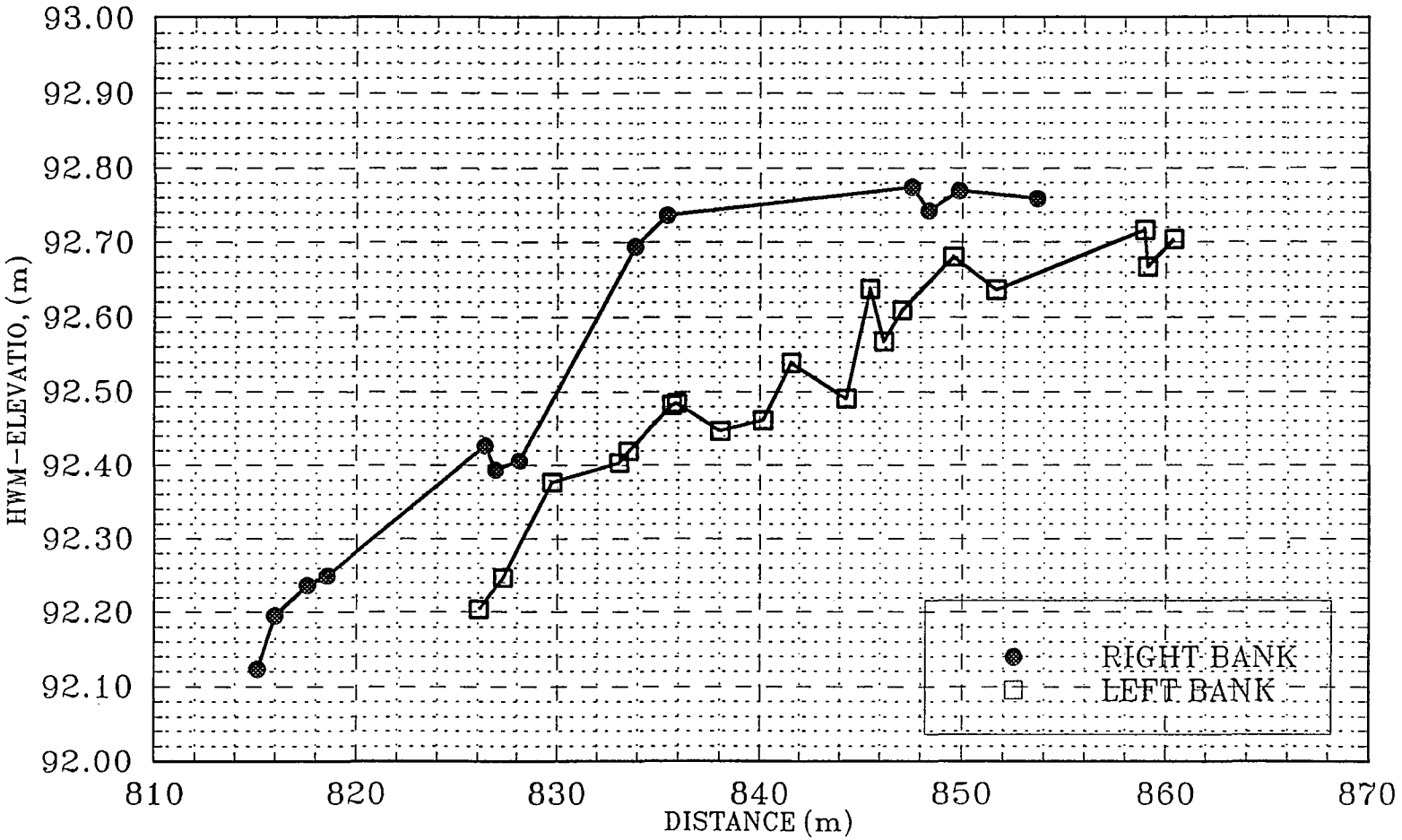

X-SEC. 1 DOWNSTREAM FLUME 9
(FLOOD OF AUGUST 31, 1993)

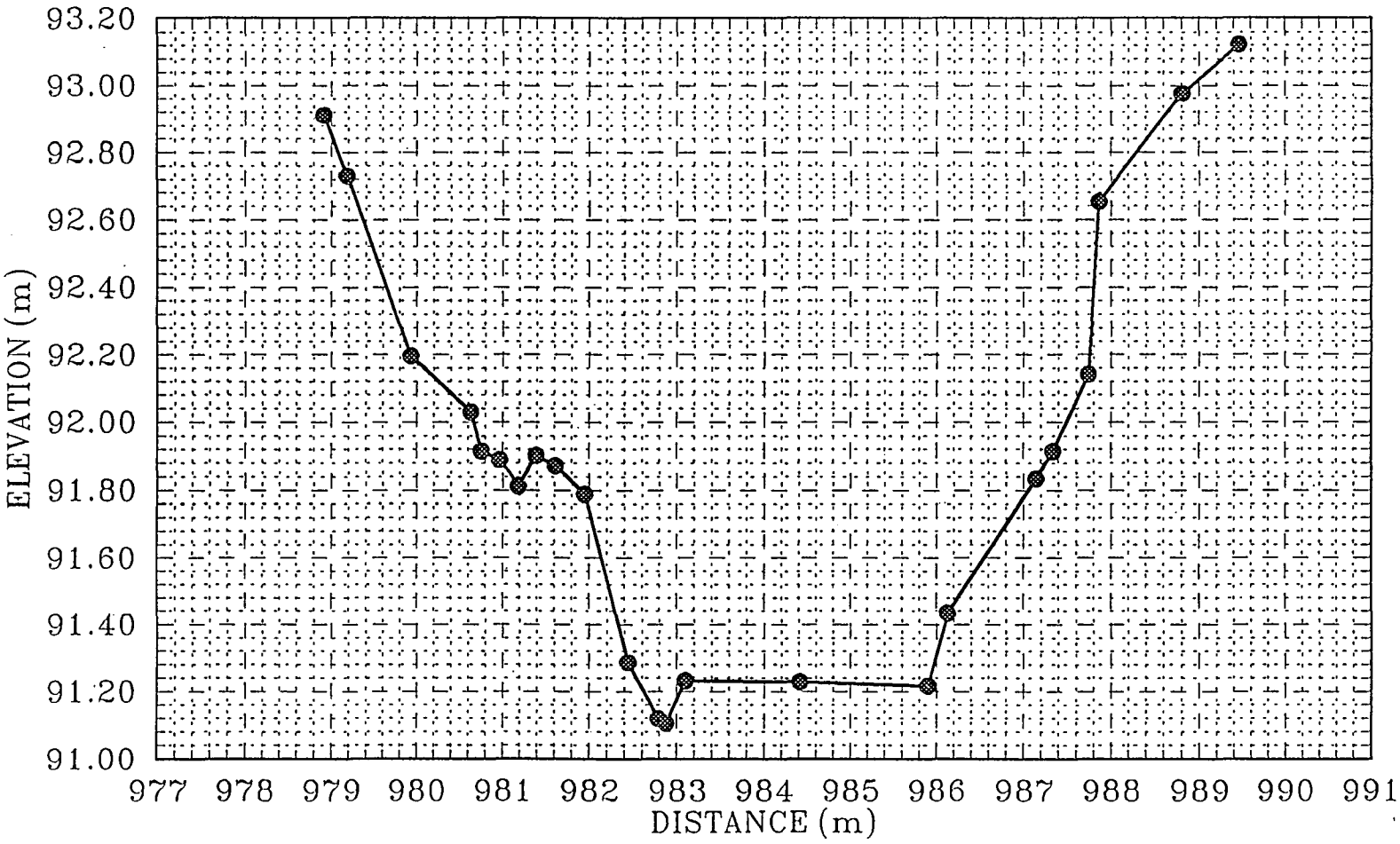

X-SEC. 2 DOWNSTREAM FLUME 9
(FLOOD OF AUGUST 31, 1993)

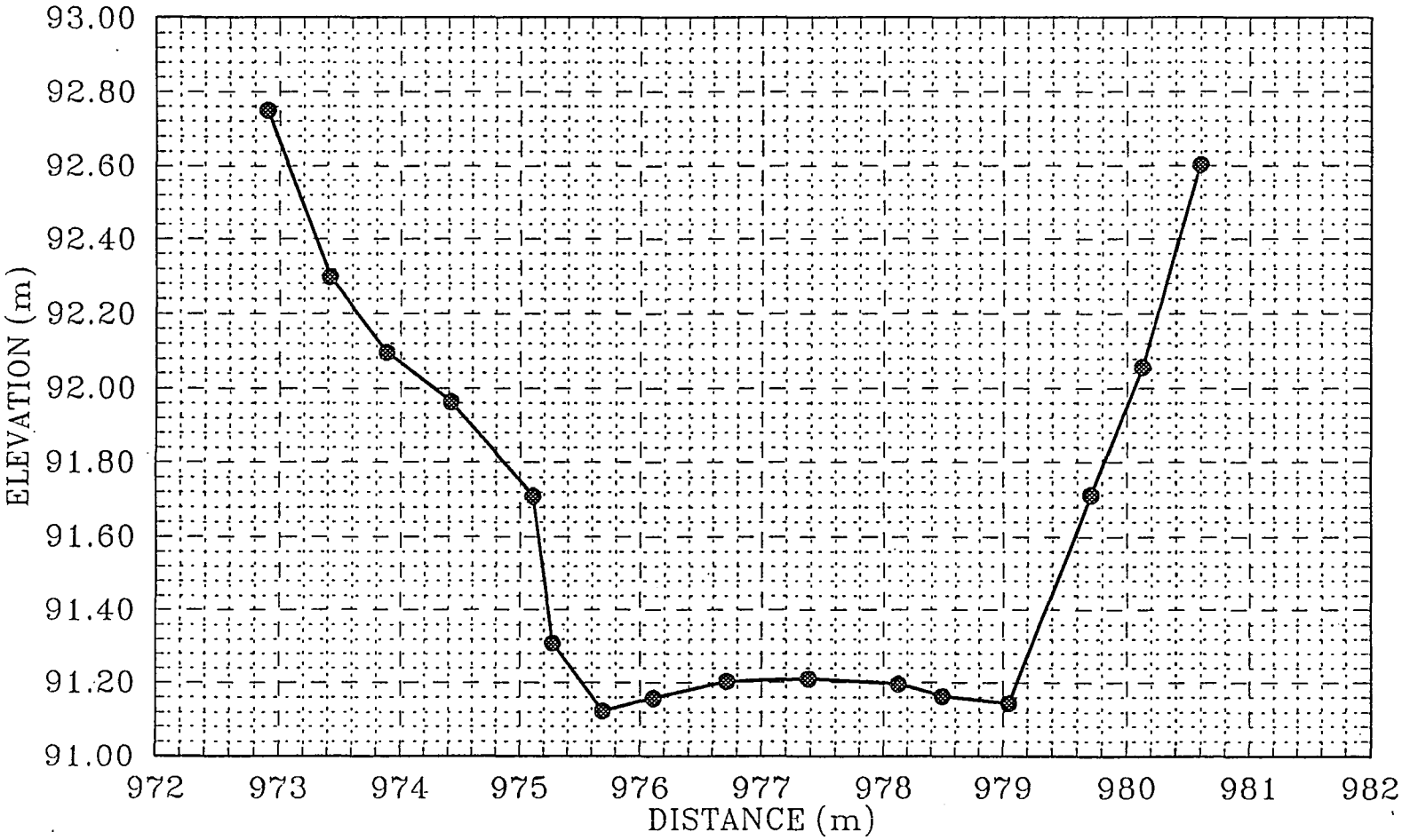

X-SEC. 3 DOWNSTREAM FLUME 9
(FLOOD OF AUGUST 31, 1993)